

that may be relevant to future revisions of the Yucca Mountain Biosphere Process Model. Despite the difference in climatic conditions and the accident/potential-exposure scenarios for Chernobyl and Yucca Mountain, respectively, the Chernobyl data serve as a source of information to improve the confidence in a conceptual model of exposure pathways and process models. As part of the biosphere-model validation for both groundwater release and volcanic release scenarios, the YMP is interested in measurements that could represent input data in validating models for specific environmental processes, as listed in Section 13.2. The main conclusions that can be drawn from Chernobyl with respect to these processes and parameters are described below.

Radionuclide transfer from soil to plant via root uptake (see Section 13.3.8.2). Cesium migration from soils to grasses is relatively rapid. The radionuclide migration from roots into the tree trunks is limited by diffusion and advective radionuclide transfer from the soil (Bulgakov and Konoplev 2000 [156699]). Root uptake became a significant contributor to the food chain in the second year after the accident (Prister et al. 1991 [157548], p. 146).

Radionuclide transfer from soil to plants via atmospheric resuspension, including deposition of resuspended material on plant surfaces (see Section 13.3.5). Resuspension of radionuclides by wind-driven dust is an important factor after the tillage of agricultural lands, increasing the resuspension by more than an order of magnitude. Resuspended material is likely to settle on plant surfaces, thereby increasing their contamination. The Chernobyl data on hot-particle dispersal and dust transport showed that radionuclides attach to dust particles and move as combined particles. Aspects of models of atmospheric contaminant dispersal, radionuclide fallout, radionuclide resuspension, and particle-size distributions developed by Garger et al. (1999 [151483]), Goldman et al. (1987 [156820]), and Kashparov et al. (2000 [156622]) may be relevant to building confidence in a model for radionuclide resuspension resulting from a volcanic eruption through a potential Yucca Mountain repository.

Radionuclide transfer from animal food to animal products (see Sections 13.3.8.2 and 13.3.8.4). These data could be used in assessing the Yucca Mountain models for meat and milk contamination. Environmental half-life periods of decay of ^{137}Cs content in milk and agricultural products were shorter than those initially expected.

Removal of contaminants via erosion and leaching (see Sections 13.3.5 and 13.3.8.1). The average annual topsoil erosion in Ukraine from 1987 to 1990 contributed to the annual removal of 0.7×10^5 Bq/ha of ^{137}Cs from soils (Prister et al. 1991 [156824], Table 7). As a result of biochemical and physical-chemical processes, hot particles have been significantly dissolved by now, and radionuclides have been transferred to soils (Kashparov 2001 [156819], p. 37). The use of physical values of the half-life of radionuclides gives conservative estimates of radionuclide removal from soils in the Yucca Mountain Biosphere Process Model.

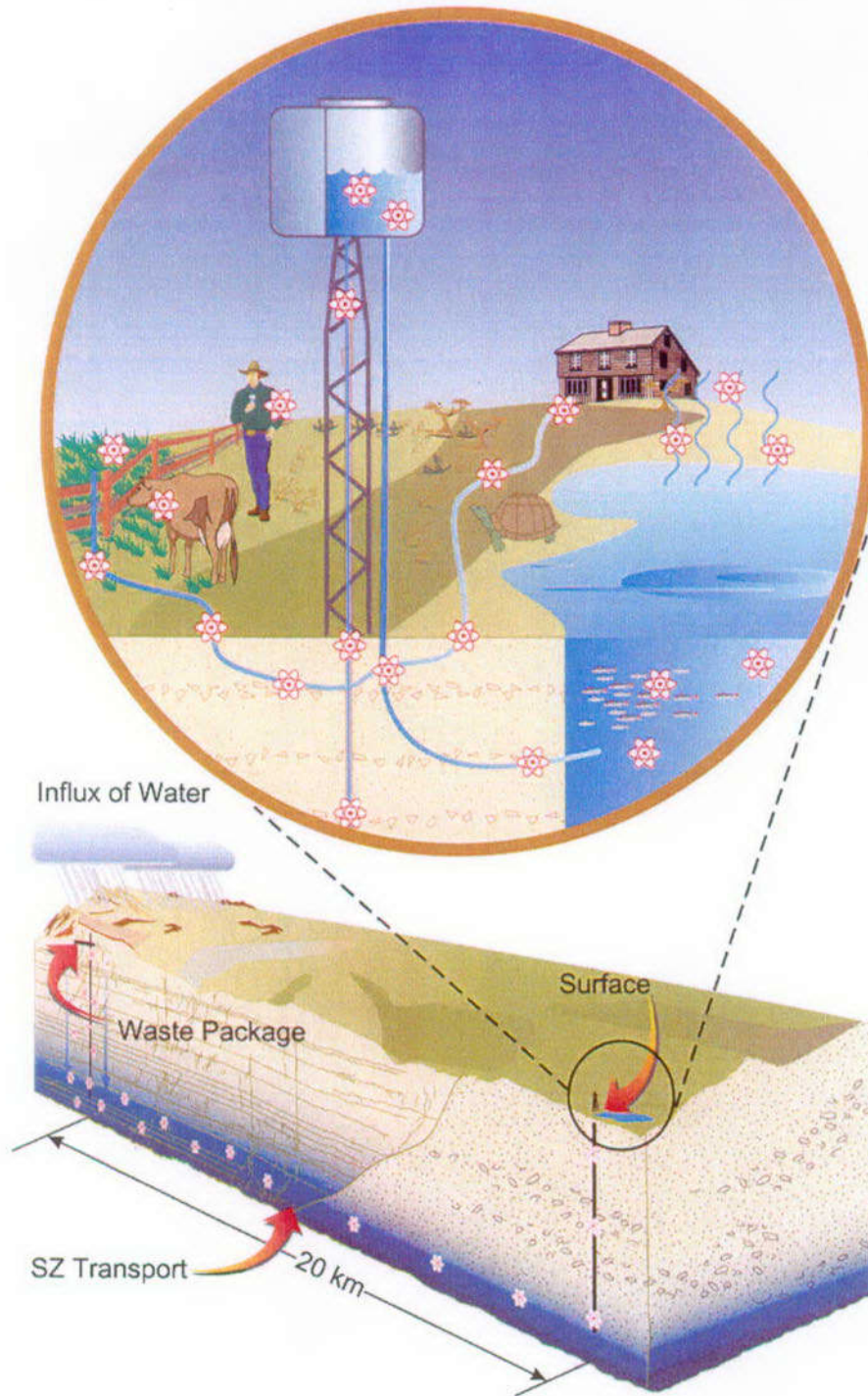
Inhalation of resuspended contamination material originally deposited on the ground (see Sections 13.3.5 and 13.3.9.3). The most hazardous particles associated with the Chernobyl accident are those containing plutonium, which can contribute up to 40% of radioactivity in the dust (Anokhova and Krivtsov 1991 [156829], p. 206). The inhalation doses for agricultural laborers are greater than the external doses, with the plutonium concentration exceeding the acceptable limit by an order of magnitude.

Radionuclide accumulation in soils and plants under irrigation using contaminated water (see Section 13.3.7). Irrigation using contaminated water creates radioactive contamination of both irrigated soils and agricultural products (Perepelyatnikov et al. 1991 [156822]; Bondar et al. 1991 [156846]). The increase in the concentration of radionuclides in soils during irrigation in the southern Ukraine, where environmental conditions are more similar to those at Yucca Mountain than are those in the Chernobyl vicinity, confirms the concept of a radionuclide-buildup factor used in the Yucca Mountain Biosphere Process Model.

In summary, results of the Chernobyl literature survey suggest that soil type influences the ecological half-life of radionuclides in the biosphere, both in regard to soil bioaccumulation factors and advective and diffusive transport properties that limit radionuclide transfer to plant roots. With respect to rural populations, agricultural methods—including irrigation and tillage—and crop types play an important role in resuspension of radionuclides. Resuspended material is likely to increase the contamination of plant surfaces. Resuspended radionuclides would increase the inhalation dose for agricultural workers, which would be particularly significant for plutonium associated with the Chernobyl accident.

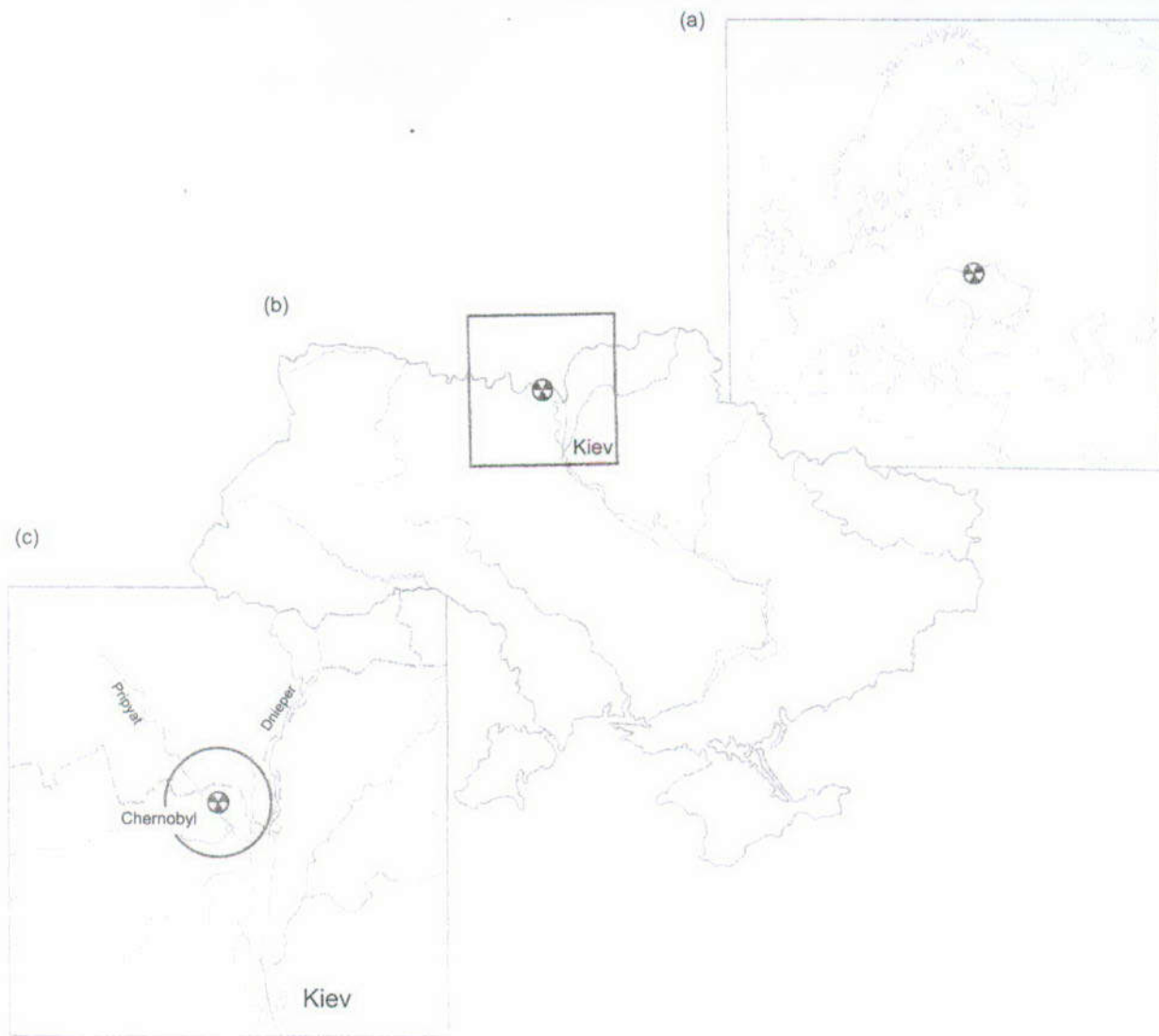
Chernobyl data include both the relatively short-lived isotopes of iodine, cesium, and strontium, and long-lived transuranic elements such as plutonium and americium. Among the long-lived radionuclides of interest to Yucca Mountain, and not present at Chernobyl, are ^{129}I , ^{227}Ac , ^{232}U , ^{233}U , ^{237}Np , ^{243}Am , ^{210}Pb , ^{231}Pa , ^{226}Ra , ^{230}Th , and ^{242}Pu (CRWMS M&O 2000 [151615], Sections 3.3.1 and 3.3.2).

Numerous data collected for the past 15 years about the distribution and accumulation of radioactive materials in different parts of the biosphere after the Chernobyl accident, including the main exposure pathways and mechanisms of radioactive contamination of the environment and the population, can be used to build confidence in Yucca Mountain conceptual and numerical models. They can also be used to enhance models for long-term transport processes and radiation doses associated with possible exposure to radioactive material in the vicinity of the potential nuclear waste disposal site at Yucca Mountain. For the potential groundwater-contamination scenario at Yucca Mountain, radionuclide-contaminated water, which is to be used as the source of drinking water, irrigation, animal watering, and domestic uses, is expected to increase the likelihood of ingestion uptake of radionuclides by humans. Chernobyl data on the atmospheric distribution of contaminants, their fallout, and redistribution in soils and plants may be considered an anthropogenic analogue for the potential release of radionuclides caused by a volcanic eruption at Yucca Mountain, accompanied by atmospheric dispersal of contaminants into the environment through ash fallout on the land surface. Analogues related to volcanic processes are discussed in Section 14.



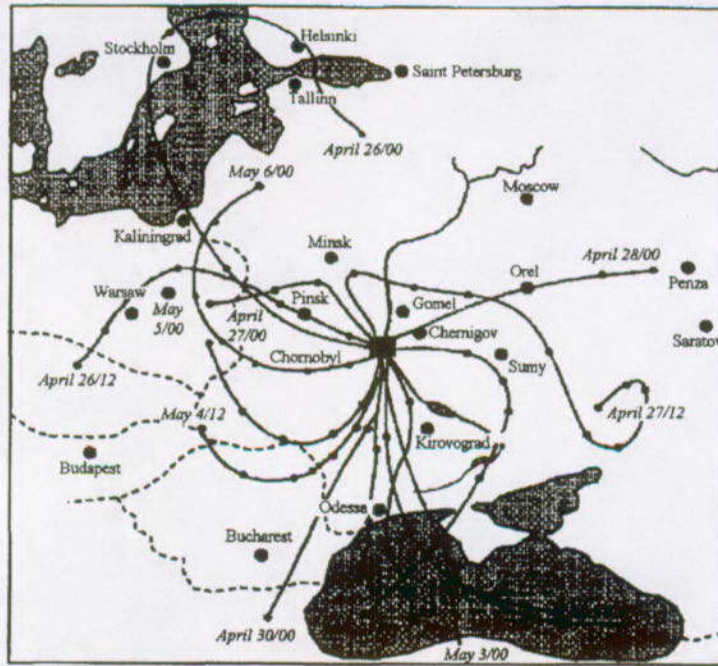
Source: CRWMS M&O 2000 [151615], Figure 3-1.

Figure 13.2-1. Illustration of the Biosphere in Relationship to the Potential Repository System



Source: Modified from Shestopalov 1996 [107844], p. 1.

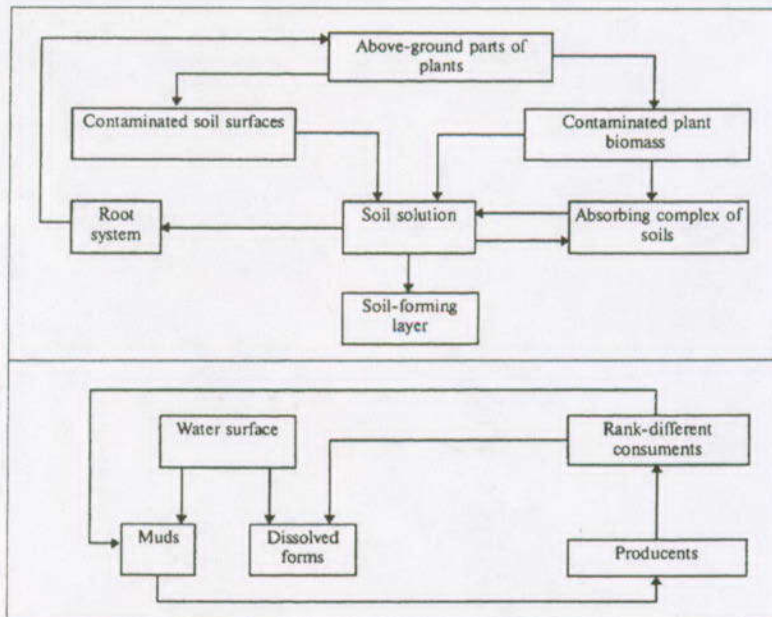
Figure 13.3-1. Location of the ChNPP in (a) Europe, (b) Ukraine, and (c) the Kiev Region



NOTE: Dashed lines indicate country boundaries, and Dates/Times indicate date and time (in hours) in 1986.

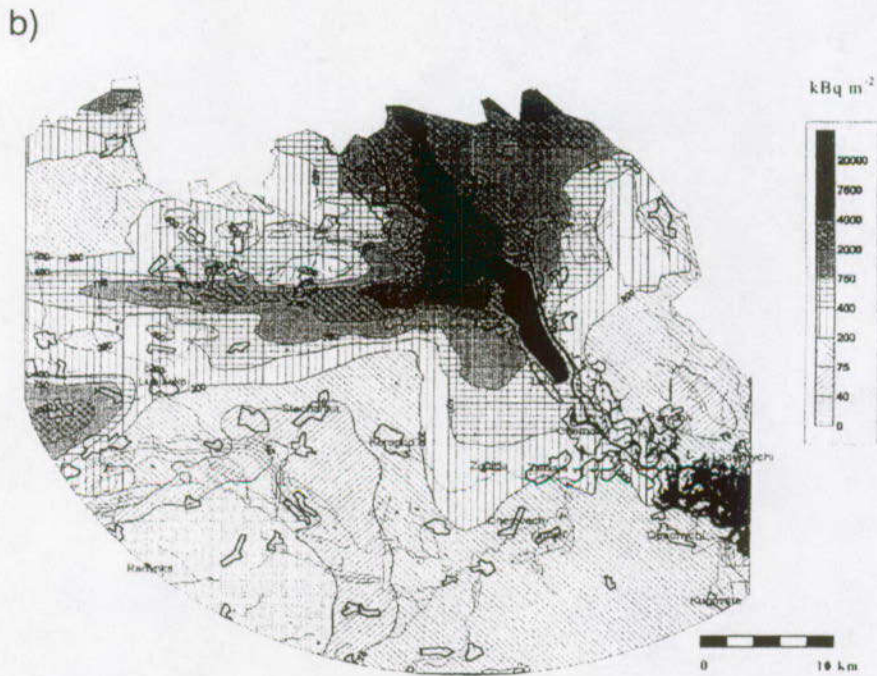
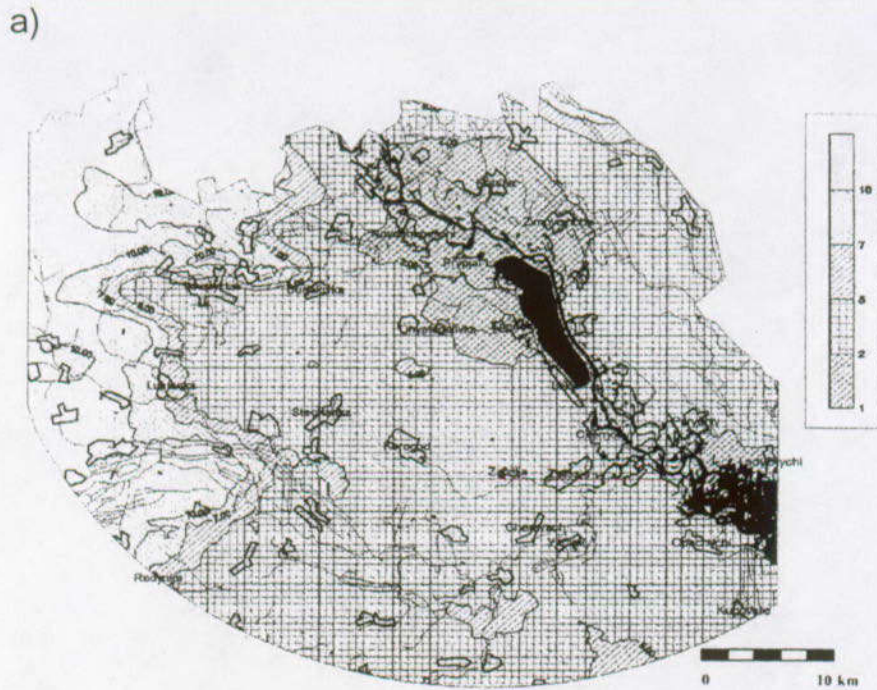
Source: Bar'yakhtar et al. 2000 [157504], Figure 2.5.2).

Figure 13.3-2. Fallout Trajectories of the ChNPP Accident



Source: Baryakhtar 1997 [156953], Figure I.3.19, p. 263.

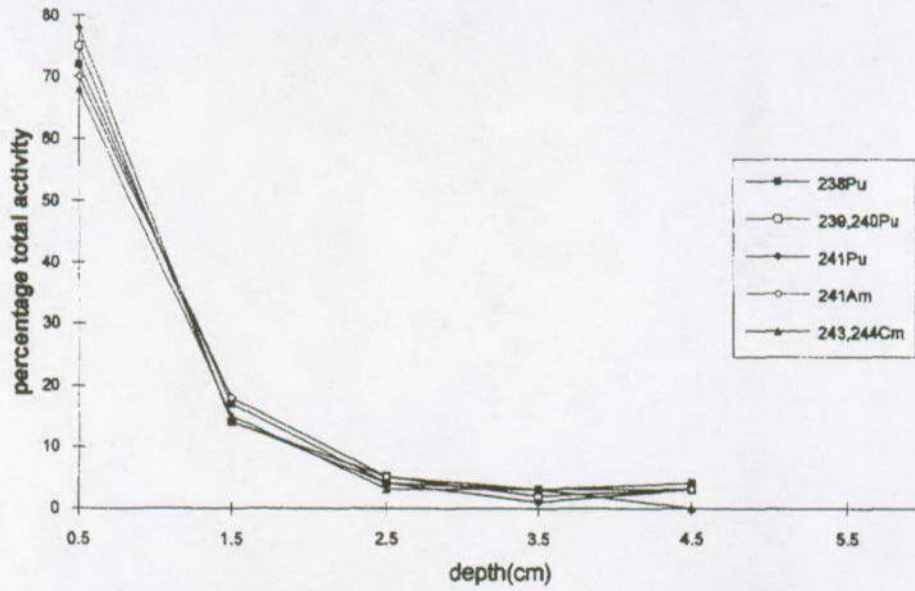
Figure 13.3-3. Schematic Illustrating the Principal Pathways for the Radionuclides Entering the Biosphere through Terrestrial and Aquatic Ecosystems That Were Considered in Evaluating the Consequences of the Chernobyl Accident



NOTE: Concentrations are kBq/m².

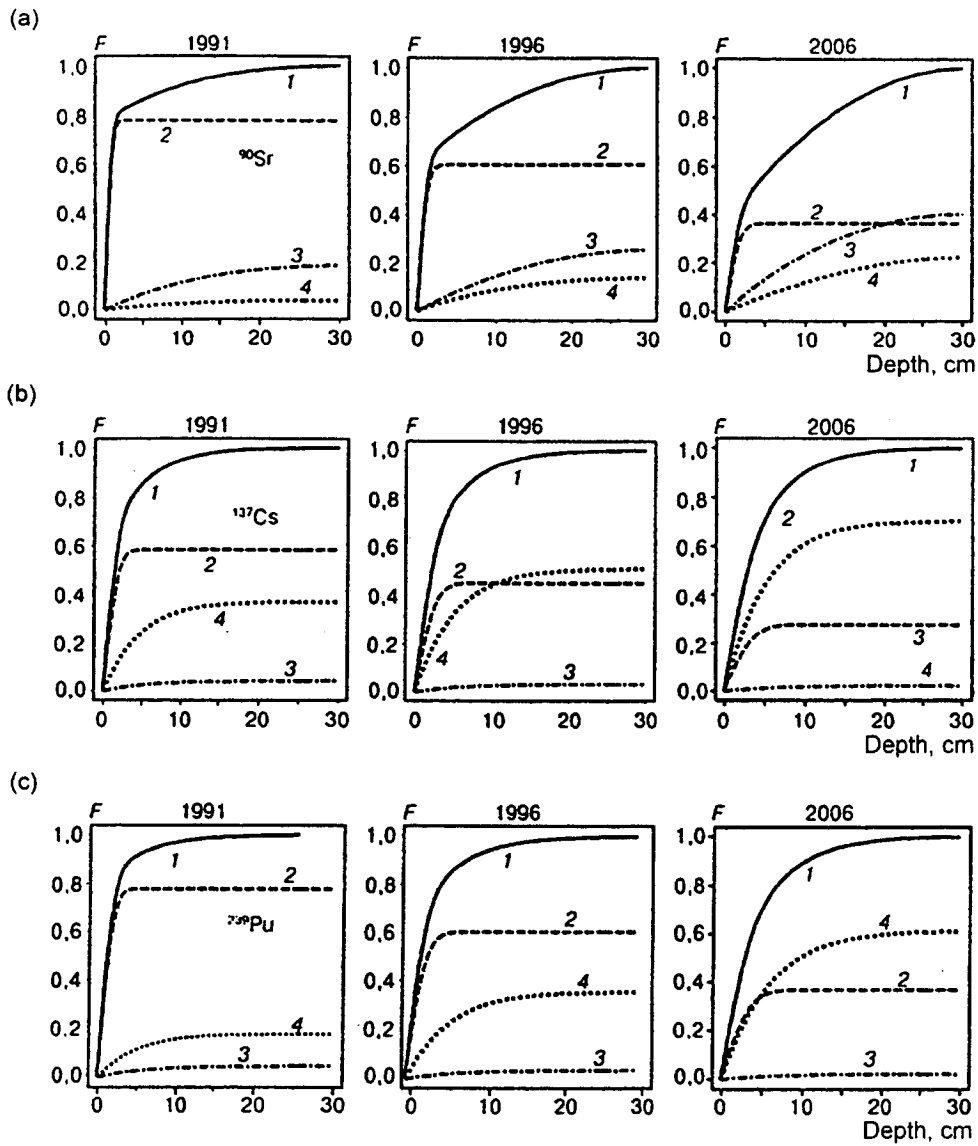
Source: Data of the Ukrainian Institute of Agricultural Radioecology (Kashparov et al. 2001 [157400], Figure 3, Figure 2).

Figure 13.3-4. Maps of the Terrestrial Contamination of the 30 km Chernobyl Exclusion Zone in Ukraine: (a) ⁹⁰Sr; (b) ¹³⁷Cs



Source: Mboulou et al. 1998 [156628], Figure 1.

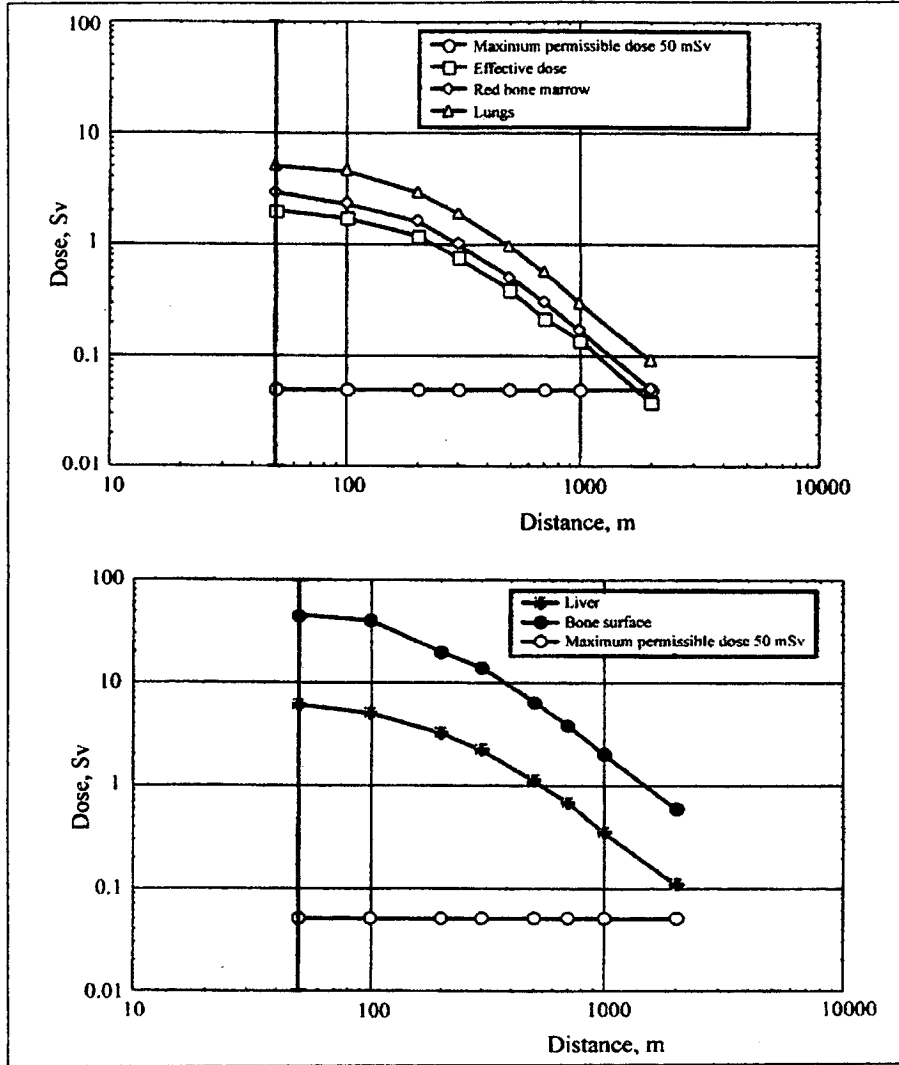
Figure 13.3-5. Vertical Distribution of Actinides in Soil to 4.5 cm



NOTE: 1 - total content, 2 - radionuclides in fuel particles, 3 - mobile forms, and 4 - absorbed forms.

Source: Ivanov 2001 [156818], p. 57.

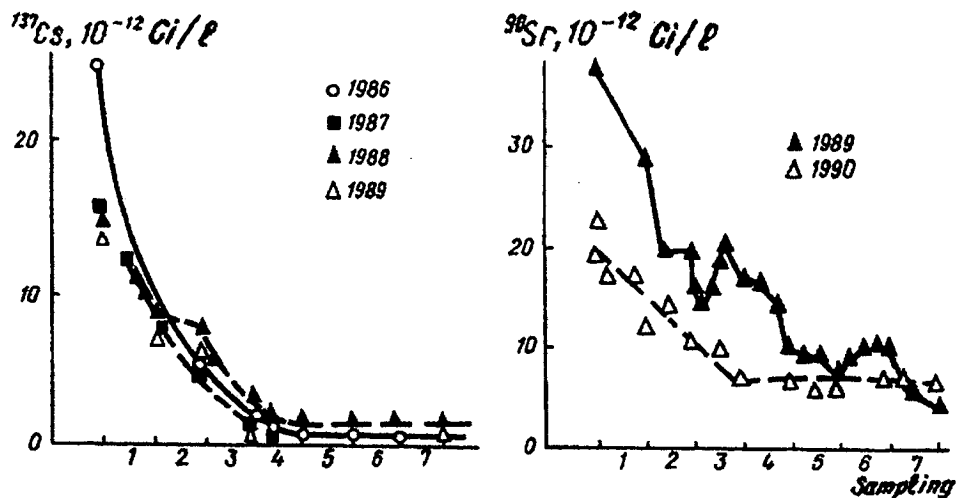
Figure 13.3-6. Dynamics of Redistribution of ^{90}Sr (a), ^{137}Cs (b), and ^{239}Pu (c) as a Function of Depth and Time in Derno-podzolic Silt Soils



NOTE: For Pasquill weather Category C with no wind and speed of 4.2 m/s at 100 m altitude, which corresponds to a wind speed of 2.53 m/s at the surface.

Source: Bar'yakhtar et al. 2000 [157505], Figure 3.5.2.

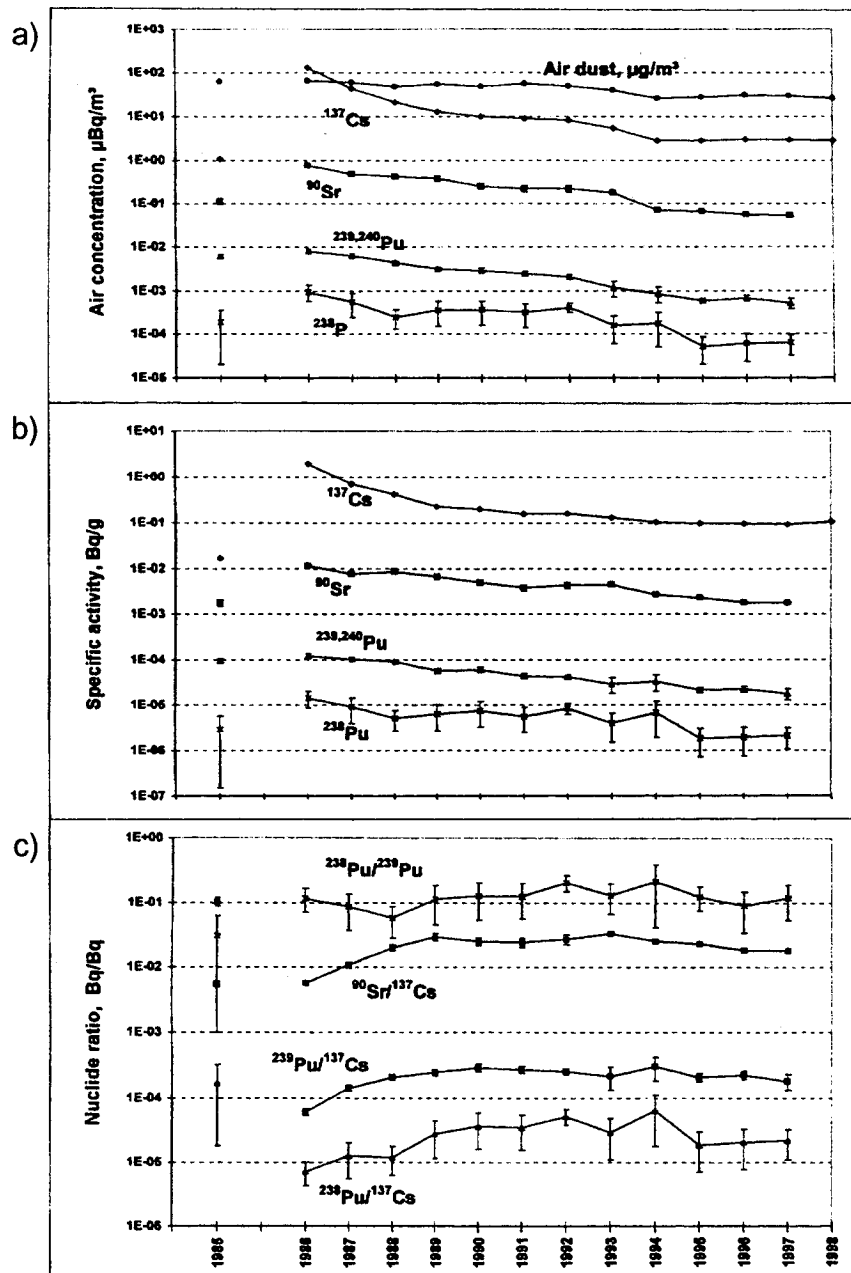
Figure 13.3-7. Predicted Inhalation Doses as a Function of the Distance from the Hypothetical Collapsed Shelter



NOTE: 1: mouth of Pripyat; 2: Kiev Reservoir; 3: Kanev Reservoir; 4: Kremenchug Reservoir; 5: Dneprodzerzhinsk Reservoir; 6: Zaporozh'e Reservoir 7: Kakhovka Reservoir.

Source: Modified from Bar'yakhtar 1997 [156953], Figure I.3.16, p. 250.

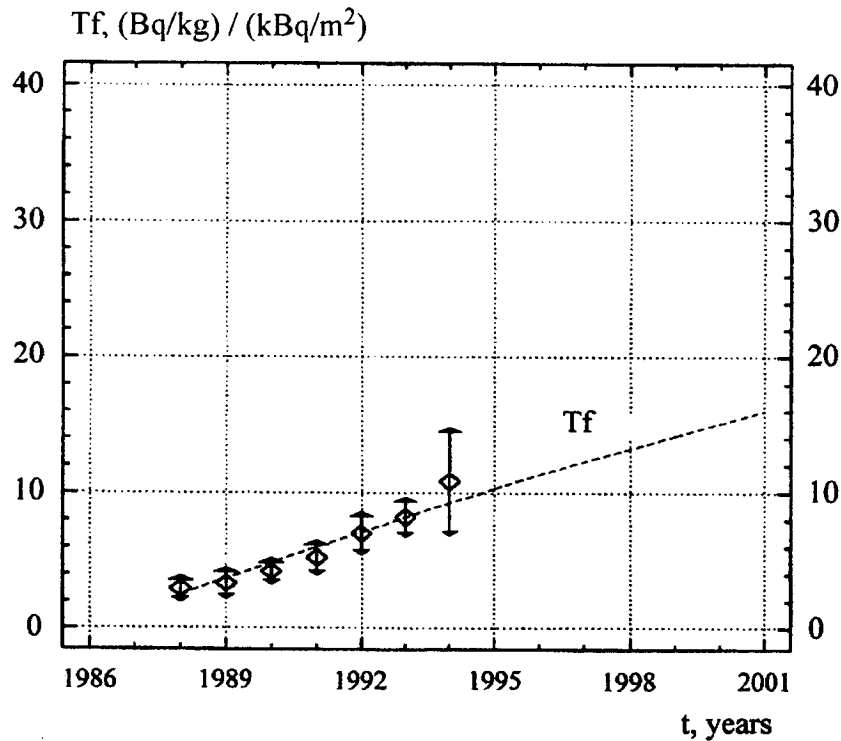
Figure 13.3-8. Concentration of ^{90}Sr and ^{137}Cs in Water from Seven Sites along the Dnieper River



NOTE: All values are corrected for radioactive decay to 1 May 1986. Values for 1986 relate to the second half of the year only, i.e., the Chernobyl deposition phase is not included. The air-dust concentration ($\mu\text{g}/\text{m}^3$) is shown for comparison.

Source: Rosner and Winkler 2001 [156629], Figure 1.

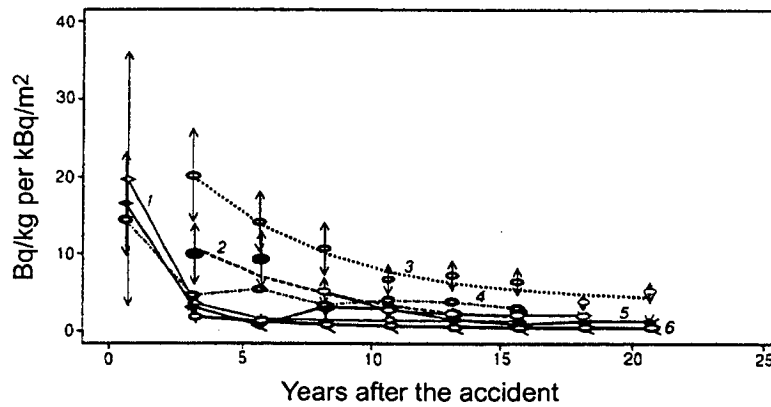
Figure 13.3-9. Mean Values of (a) Radionuclide Concentrations in Air ($\mu\text{Bq}/\text{m}^3$), (b) Specific Activities in Air Dust (Bq/g), and (c) Radionuclide Ratios in Air (Bq/Bq) at Munich-Neuherberg Since 1985.



NOTE: Data points are experimental values; the line is the theoretical curve for pH=6.

Source: Bar'yakhtar et al. 2000 [157504], Figure 2-5.9.

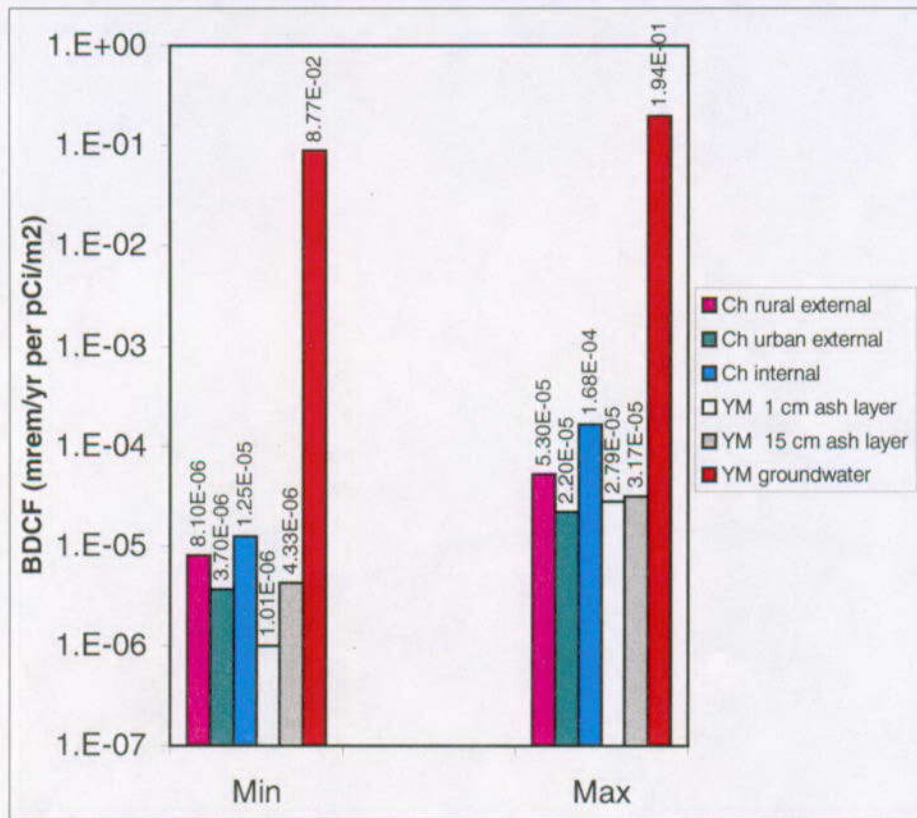
Figure 13.3-10. Effective Meadow-Vegetation Transfer Coefficients for ⁹⁰Sr (T_f), Neglecting Redistribution in the Root Layer



NOTE: 1, 2: derno-podzolic sandy soils; 3: derno-podzolic silty and sandy soils; 4: mineral soils with fuel traces; 5: derno-podzolic sandy soils with fuel traces; 6: loamy and clayey soils.

Source: Ivanov 2001 [156818], Figure 10, p. 63 (summarized the results of several authors).

Figure 13.3-11. Dynamics of the Soil-Plant Transfer Coefficient for ¹³⁷Cs, Which Is Approximated by a Function $y = a \exp(-bt) + (1-a) \exp(-ct)$, for Meadow Grass Areas

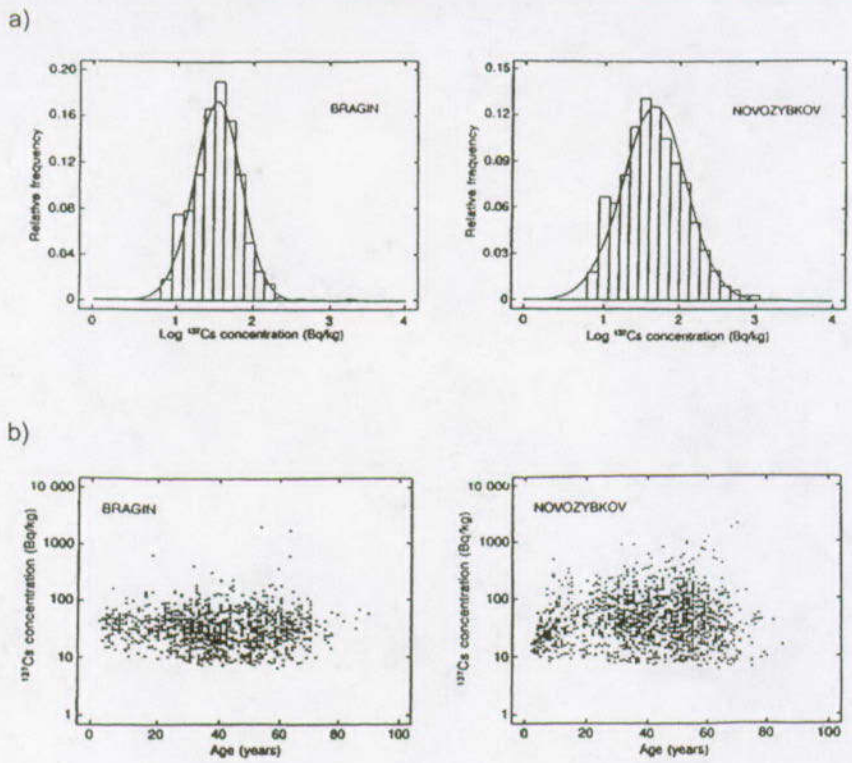


NOTE: For groundwater BDCF, refer to Section 13.3.9.2.

Chernobyl External Dose (Table 13.3-10b); Yucca Mountain (YM) Disruptive Event Contamination Scenario (Table 13.3-10c); and Internal Radiation for Soil Types for Chernobyl (Table 13.3-11).

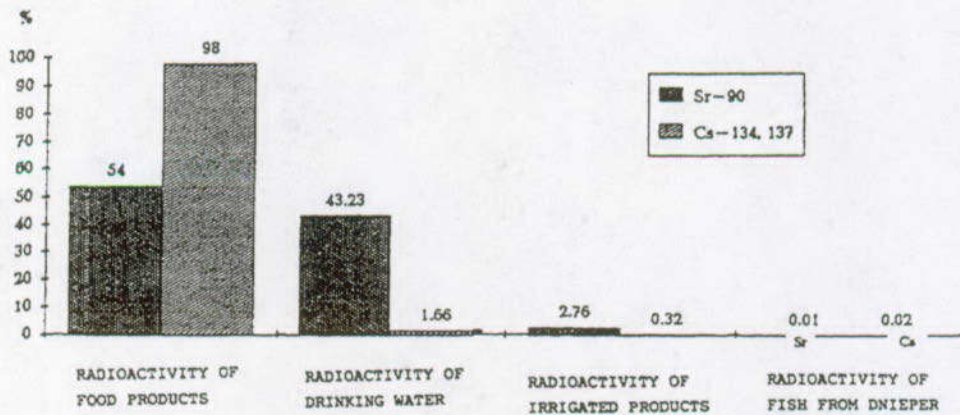
Source: CRWMS M&O 2000, [151615], Table 3-17 (for Yucca Mountain Groundwater Contamination Scenario).

Figure 13.3-12. Comparison of Minimum and Maximum Values of ¹³⁷Cs BDCFs for Chernobyl (Ch) and Yucca Mountain



Source: (a) IAEA (International Atomic Energy Agency) 1991 [156750], p. 265;
 (b) IAEA 1991 [156750], p. 263.

Figure 13.3-13. (a) Frequency Distributions of the Logarithm of ¹³⁷Cs Concentration in the Body at Two Selected Settlements (Bragin, Belarus, and Novozybkov, Russia); (b) Scatter Diagram of ¹³⁷Cs Concentration in the Body as a Function of Age



Source: Voitsekhovitch et al. 1996 [156921], Figure 8.

Figure 13.3-14. Contribution of ⁹⁰Sr and ¹³⁷Cs in Different Components of Food Chain Pathways to Averaged Effective Internal Dose for the Population of the City of Kiev (1993 scenario)

Table 13.3-1. Vertical Distribution of Plutonium and Uranium in Soils in the Vicinity of the ChNPP

Depth (cm)	^{239(240)Pu} (%)	Ratio ^{238U} / ^{235U}
0-1	91-97	79.9-103.5
1-2	2.9-7.9	126.7-135.8
2-3	0.3-0.6	129.6-137.3
3-4	0-0.2	137.1-137.8
4-5	0-0.1	137.6-137.8

Source: Sobotovich 1992 [134218], Table 3.6.

Table 13.3-2. Typical Radioactive Contamination Levels (Bq/L) for Groundwater in the Inner Exclusion Zone

Source of water	^{90Sr}	^{137Cs}	^{239+240Pu}	^{241Am}
MPC (maximum permissible concentration)	14.8	555.5	81.5	70.3
Regional groundwater contamination	0.1-10	0.1-1	≤0.01	≤0.01
Shelter	10-10 ³	0-100	--	--
Interim radioactive waste storage sites	10 ² -10 ⁴	0.1-10	≤0.01-1	≤0.01
Cooling pond	1-10 ²	0.1-1	--	--
Artesian aquifer in Eocene deposits	≤0.01	≤0.01	--	--

Source: Shestopalov and Poyarkov 2000 [157507], Table 5.4.1.

Table 13.3-3. Percentages of Measured Concentrations of Radionuclides in Kiev Metropolitan Area Groundwater, 1992–1996

Aquifer	^{137Cs} Concentration, mBq/L				^{90Sr} Concentration, mBq/L		
	<10	10–50	51–150	>150	<10	10–50	>50
Quaternary	24%	56%	14%	6%	53%	40%	7%
Eocene	45%	41%	9%	5%	71%	21%	8%
Late Cretaceous (Cenomanian)–Early Jurassic (Callovian)	46%	31%	13%	10%	80%	20%	--
Middle Jurassic (Bajocian)	47%	28%	15%	10%	62%	35%	3%

NOTE: The depths tested are: Quaternary aquifer: 2–18 m; Eocene aquifer: 45–65 m; Late Cretaceous (Cenomanian)–Early Jurassic (Callovian) aquifer: 80–150 m; Middle Jurassic (Bajocian) aquifer: 200–300 m.

Source: Shestopalov and Poyarkov 2000 [157507], p. 150, Table 5.4.2.

Table 13.3-4. Cesium-137 Concentrations in Agricultural Products Grown on Lands Irrigated Using Water from the Dnieper River Reservoirs, Compared with Lands Irrigated by Water from Other Sources

Type of Plant	Year	Irrigation using Contaminated Water from Dnieper River Reservoirs (see Figure 13.3-8)				Irrigation Using Uncontaminated Water	
		Kanev	Kremenchuh	Dnepro-dzerzhinsk	Kakhovka	Kharkov Region	Donetsk Region
Winter wheat (seeds)	1987	50	50	25	30	8	10
	1988	30	40	10	30	10	10
Corn (seeds)	1987	10	10	5	6	2	2
	1988	10	5	6	3	1	2
Alfalfa	1987	600	600	370	320	80	100
	1988	400	400	300	200	90	90
Cabbage	1987	6	7	3	3	1	1
	1988	6	4	2	3	1	1
Tomato	1987	20	20	10	10	4	5
	1988	20	10	10	20	6	5
Tomato (vegetative mass)	1987	700	800	500	400	160	250
	1988	400	500	200	200	200	200
Cucumber	1987	40	40	20	20	10	10
	1988	30	40	20	10	10	20
Cucumber (vegetative mass)	1987	1,200	1,600	800	600	350	300
	1988	800	1,100	400	300	300	200

NOTE: ¹³⁷Cs reported as pCi/kg of air-dry mass

Source: Pereplyatnikov et al. 1991 [156822], p. 111, Table 5.

Table 13.3-5. Distribution of (a) ¹³⁷Cs and (b) ⁹⁰Sr in the Soil Profile beneath Rice Paddies in 1988 after Three Years of Irrigation, Southern Ukraine

a) ¹³⁷Cs (in pCi/kg of air-dry soil)

Soil layer (cm)	Year	Type of Agriculture					
	1986	Bare	Rice	Fallow	Alfalfa	Rice	Rice
	1987	Bare	Alfalfa	Rice	Fallow	Fallow	Rice
	1988	Bare	Fallow	Alfalfa	Rice	Rice	Rice
0-0.5		0.45	0.41	0.52	0.6	0.62	0.71
0.5-2		0.43	0.39	0.39	0.51	0.5	0.49
2-4		0.4	0.4	0.37	0.41	0.38	0.37
4-6		0.38	0.36	0.4	0.38	0.42	0.41
6-8		0.43	0.45	0.42	0.37	0.39	0.42
8-10		0.37	0.37	0.38	0.38	0.37	0.32
10-20		0.19	0.4	0.39	0.41	0.4	0.41
Average in a layer 0-20 cm		0.37	0.4	0.42	0.44	0.45	0.48
Contamination (Ci/km ²)		0.11	0.12	0.12	0.13	0.14	0.14

b) ⁹⁰Sr (in pCi/kg of air-dry soil)

Soil Layer (cm)	Year	Type of Agriculture					
	1986	Bare	Rice	Fallow	Alfalfa	Rice	Rice
	1987	Bare	Alfalfa	Rice	Fallow	Fallow	Rice
	1988	Bare	Fallow	Alfalfa	Rice	Rice	Rice
0-0.5		70	--	--	--	110	120
0.5-2		65	--	--	--	110	110
2-4		60	--	--	--	100	122
4-20		58	--	--	--	100	115
Average in a layer 0-20 cm		60	--	--	--	102	116
Contamination (Ci/km ²)		0.018	--	--	--	0.031	0.035

Source: Perepelyatnikov et al. 1991 [156822], pp. 109-110, Tables 2 and 3.

Table 13.3-6. Estimated Soil-to-Plant Transfer Factors for Yucca Mountain Compared with Those Determined from Observations After the Chernobyl Accident

Radionuclide	Soil-to-Plant Transfer Factors (Dimensionless)				
	Yucca Mountain				Chernobyl data
	Leafy	Root	Fruit	Grain	
Strontium	2.0E+00	1.2E+00	2.0E-01	2.0E-01	2.0E-02-1.2E+01
Yttrium	1.5E-02	6.0E-03	6.0E-03	6.0E-03	(3-70) x E-03
Cesium	1.3E-01	4.9E-02	2.2E-01	2.6E-02	2.0E-02-1.1E+00
Radium	8.0E-02	1.3E-02	6.1E-03	1.2E-03	(1-40) x E-03
Thorium	4.0E-03	3.0E-04	2.1E-04	3.4E-05	(1-700) x E-03
Uranium	8.5E-03	1.4E-02	4.0E-03	1.3E-03	1.6E-03-1.0E-01*
Neptunium	3.7E-02	1.7E-02	1.7E-02	2.7E-03	nE-02-nE-01**
Plutonium	3.9E-04	2.0E-04	1.9E-04	2.6E-05	nE-08-1.0E+00
Americium	2.0E-03	4.7E-04	4.1E-04	9.0E-05	nE-06-1.0E-01

NOTE: * Data are for ²³⁸U; **n = any number from 1 to 10

Source: Bar'yakhtar 1997 [156953], p. 271 for Chernobyl; CRWMS M&O 2000 [151615], Table 3-10 for Yucca Mountain.

Table 13.3-7. Soil-to-Fodder Transfer Coefficients Determined after the Chernobyl Accident for ¹³⁷Cs

Crop	Soil Type and pH		
	Derno-podsol pH=4.5-5.5	Gray Forest pH=5.6-6.5	Chernozem pH=6.6-7.2
Hay from natural grass	10	4	1.8
Hay from planted grasses	4	3	1.6
Vetch	2.7	0.45	0.2
Clover	1.8	0.3	0.3
Lupine	1.5	0.4	0.15
Alfalfa	0.8	0.4	0.2
Silage	0.4	0.2	0.08
Fodder beet	0.5	0.35	0.2
Potato	0.25	0.13	0.045
Winter grain	0.5	0.2	0.05
Rye	0.4	0.1	0.04
Barley	0.3	0.1	0.06

NOTE: ¹³⁷Cs reported as (Bq/kg) / (kBq/m²) (mean for 1987-1990).

Source: Shestopalov and Poyarkov 2000 [157507], p. 174, Table 5.6.2

Table 13.3-8. Concentrations of ¹³⁷Cs in Pasture, Meat and Milk, and Calculated Transfer Coefficients

Pasture Contamination (Bq/kg)	Intake* (kBq/day)	Meat (Bq/kg)	Milk (Bq/kg)	Transfer coefficients	
				Meat (day/kg)	Milk (day/L)
250	17.5	280	112	1.6E-02	6.4E-03
500	36	700	280	1.9E-02	7.8E-03
1,000	70	1,400	550	2.0E-02	7.9E-03
1,500	105	2,100	840	2.0E-02	8.0E-03
2,000	140	2,800	1,120	2.0E-02	8.0E-03
3,000	210	4,200	1,680	2.0E-02	8.0E-03
5,000	350	7,000	2,800	2.0E-02	8.0E-03
10,000	700	14,000	5,600	2.0E-02	8.0E-03

NOTE: *Assumes daily intake of 70 kg fresh herbage/animal. For comparison, in the Yucca Mountain biosphere model, the dairy and beef cow feed consumption rates are 55 and 68 kg/day, respectively (CRWMS M&O [151615], Table 3-13).

Source: Richards and Hance 1996 [157613]. Only equilibrium concentrations are included in the table.

Table 13.3-9. Example of the Database to Assess Radiation Dose for the City of Bragin, Belarus

Population						
Population Group	1986	1987	1988	1989	1990	
Children	1,667	--	--	2,065	--	
Total inhabitants	5,600	4,900	--	5,888	--	
Deposition Density (kBq/m ²)						
Radionuclide	1986	1987	1988	1989	1990	
Cesium-137	1,700	1,000	270 (5-1,000) ¹⁾ (n = 8) ²⁾	1,000 (n = 18) 830 (n = 50)	--	
Strontium-90	--	--	--	78 (n = 9)	--	
Exposure Rate (µR/h)						
	1986	1987	1988	1989	1990	
Measurement	8,000 (10 May)	680 (10 May)	--	--	--	
Concentration in Foods (Bq/kg) (approximate median values) (Data from Institute of Agricultural Radiology, Gomel)						
	1986	1987	1988	1989	1990	
Milk	1,600	1,500	220	300	260	
Root vegetables	740	630	330	370	370	
Green vegetables	3,700	740	370	300	220	
Vegetables/fruit	1,100	590	300	220	330	
Berries, mushrooms	2,200	1,100	1,300	2,600	1,100	
Honey	1,300	1,900	1,500	300	300	
Eggs	1,300	190	190	190	300	
Meat	1,700	1,100	740	260	300	
Fish	--	1,800	740	1,500	220	
Consumption Rate (g/day)						
Food Item	Rural settlement		All Belarus			
Milk	735		690-710			
Bread, white	220		240			
Bread, dark	350		350			
Potatoes	540		680			
Vegetables	190		240			
Fruit, berries	160		150			
Berries	--		1.5			
Mushrooms	6		7			
Meat	150		180			
Fish	46		60			
Internal Dose (mSv) (Data for 1986, 1987: Institute of Biophysics, Moscow; data for 1988, 1989: Institute of Radiation Medicine, Minsk)						
¹³⁴ + ¹³⁷ Cs		1986	1987	1988	1989	1990
Average	Children	2 (n = 292)	1 (n = 94)	0.2 (n = 203)	0.1 (n = 3)	--
	Teenagers	5 (n = 87)	3 (n = 131)	0.2 (n = 731)	0.1 (n = 3)	--
	Adults	4 (n = 683)	3 (n = 111)	0.3 (n = 641)	0.2 (n = 131)	--
Maximum	Children	15	7	--	--	--
	Teenagers	22	17	--	--	--
	Adults	12	8	--	--	--
90 th percentile	Children	10	5	--	--	--
	Teenagers	13	7	--	--	--
	Adults	8	5	--	--	--

NOTE: ¹⁾ Range
²⁾ Number of measurements

Source: IAEA 1991 [156750], Part E, Table 2-1.

Table 13.3-10a. Dynamics of the Effective Dose of External Radiation to Ukrainians from ¹³⁷Cs Contamination after the Chernobyl Accident

Population group	Year										
	1986*	1987	1988	1989	1990	1991	1992	1993	1994	1995	1996
Urban	6.0	1.5	1.4	1.4	1.3	1.3	1.2	1.2	1.1	1.0	1.0
Rural	14.3	3.5	3.4	3.3	3.2	3.1	3.0	2.7	2.5	2.4	2.2

NOTE:* 1986 data were estimated after the accident. ¹³⁷Cs reported for 1986–1996, μSv/(kBq/m²)

Source: Los' and Poyarkov 2000 [157508], Table 6.2.1, p. 187.

Table 13.3-10b. Calculated BDCFs for ¹³⁷Cs after the Chernobyl Accident

Population group	Year										
	1986	1987	1988	1989	1990	1991	1992	1993	1994	1995	1996
Urban	2.2E-05	5.6E-06	5.2E-06	5.2E-06	4.8E-06	4.8E-06	4.4E-06	4.4E-06	4.1E-06	3.7E-06	3.7E-06
Rural	5.3E-05	1.3E-05	1.3E-05	1.2E-05	1.2E-05	1.1E-05	1.1E-05	1.0E-05	9.3E-06	8.9E-06	8.1E-06

NOTE: See Section 13.3.9.2. Units in mrem/yr per pCi/m²

Source: Table 13.3-10a.

Table 13.3-10c. Yucca Mountain BDCFs for ¹³⁷Cs for the Disruptive Event Scenario for the Transition Phase, 1 cm and 15 cm Ash Layers and Annual Average Mass Loading

BDCFs	1-cm ash layer	15-cm ash layer
	mrem/yr per pCi/m ²	mrem/yr per pCi/m ²
Mean	1.86E-06	5.81E-06
Min	1.01E-06	4.33E-06
Max	2.79E-05	3.17E-05

Source: Modified from CRWMS M&O 2001 [152536], Tables 11 and 13.

Table 13.3-11. Maximum ¹³⁷Cs Concentrations in Soils Producing Internal Dose of 1 mSv/yr and Calculated BDCFs

1	2	3	4	5	6	7
Soil Type	Concentration kBq/m ²		Concentration pCi/m ²		BDCF mrem/yr per pCi/m ²	
	Meadow	Tilled	Meadow	Tilled	Meadow	Tilled
Peat-bog	22	93	594,594	2,513,511	1.68E-04	3.98E-05
Sandy podzolic	74	130	1,999,998	3,513,510	5.00E-05	2.85E-05
Light-gray podzolic	148	185	3,999,996	4,999,995	2.50E-05	2.00E-05
Loamy chernozem	222	295	5,999,994	7,972,965	1.67E-05	1.25E-05

Source: Shestopalov and Poyarkov 2000 [157507], Table 5.6.4.

Table 13.3-12. Comparison of the Pathway Contribution (%) of Radionuclides Determined from Observations after the Chernobyl Accident in 1993

	⁹⁰ Sr			¹³⁷ Cs		
	Meat	Leafy vegetables	Milk and milk products	Meat	Leafy vegetables	Milk and milk products
Yucca Mountain	5 (10)	34 (42)	0 (2)	12 (4)	16 (3)	2 (0)
Chernobyl	4	19	54	8	2	74

Source: Yucca Mountain—CRWMS M&O 2000 [151615], Table 3-21; CRWMS M&O 2000 [151615], Table 3-24 (in parentheses)
 Chernobyl—Berkovski et al. 1996 [156592], p. 41.

Table 13.3-13. Relative Contributions to the Collective Effective Dose from ¹³⁷Cs and ⁹⁰Sr, Resulting from the Chernobyl Accident

Region/Source (%)	Irrigation	Municipal Tap Water	Fish
Kiev Region	18	43	39
Poltava Region	8	25	67
Crimean Republic *	50	50	0

NOTE: * No Dnieper River fish consumed in Crimean Republic

Source: Berkovski et al. 1996 [156592], p. 42.

Table 13.3-14. Calculated Content (Bq) of α-emitting Pu Isotopes in the Human Skeleton in 1998 for the Ukraine-Belarus Territory with Contamination Density of 20 mCi/km² (740 Bq/m²) and Comparison of These Data with Global Fallout

Type of Intake	From Global Fallout	From Chernobyl Fallout
Primary inhalation	1.3×10 ⁻³	1.2×10 ⁻²
Peroral due to superficial contamination	1.6×10 ⁻³	0.56×10 ⁻²
Peroral, biologically accessible forms	3.2×10 ⁻⁵	1.1×10 ⁻⁴
Inhalation due to resuspension	1.42×10 ⁻⁶	3.6×10 ⁻⁶
Total	2.9×10 ⁻³	1.8×10 ⁻²

Source: Bondarenko et al. 2000 [156593], Table 2.

14. ANALOGUES FOR DISRUPTIVE EVENT SCENARIOS

14.1 INTRODUCTION

This section addresses disruptive event scenarios and the ways analogues have been used to define realistic scenarios, to bound parameters in models, and to build confidence that the right processes are included in models and represented by appropriate bounding conditions. Specifically, this section addresses the disruptive event categories for volcanism and seismicity, which are considered in total system performance assessment (TSPA). The scenario for nuclear criticality has been screened out from further consideration in TSPA (DOE 2001 [153849], Section 4.3.3). However, aspects of criticality pertinent to the discussion on waste form degradation are presented in Section 4. The screened-in human-intrusion disruptive event scenario (e.g., drillhole penetrating a waste package) is not conducive to evaluation using natural analogues. Information found in Section 14.3 may help to support arguments associated with Key Technical Issue (KTI) KIA0204 listed in Table 1-1.

14.2 BACKGROUND

14.2.1 Volcanism

The Yucca Mountain stratigraphy is composed of ashfall and ash flow tuffs that were deposited approximately 13 million years ago (Ma) as a result of eruption of the Timber Mountain caldera. This large-volume, explosive, silicic volcanism ended about 7.5 Ma. Basaltic volcanism began during the latter part of the caldera-forming phase and continued into the Quaternary (the last 2 m.y.). Approximately 99% of the southwestern Nevada volcanic field, of which Yucca Mountain is a part, erupted between 15 and 7.5 Ma, with only 0.1% occurring during the basaltic phase of the last 7.5 m.y. In the Yucca Mountain region there are more than 30 basaltic volcanoes that formed between 9 Ma and 80,000 Ma. These volcanoes can be temporally and spatially separated into two distinct periods of volcanism, with the location of eruption of the younger, post-5 Ma volcanism shifted to the southwest (DOE 2001 [153849], Section 4.3.2.1.3).

To assess the probability of volcanic activity disrupting a repository, a panel of experts was assembled to conduct a volcanic hazard assessment (CRWMS M&O 1996 [100116]). The hazard analysis models are based on data from Yucca Mountain studies, along with observations from analogue studies of modern and ancient volcanic eruptions. The results of the hazard analysis estimate that 1.6×10^{-8} igneous events per year could be expected to disrupt the potential repository (CRWMS M&O 2000 [151551], Section 6.5.3 and Section 7, Tables 13 and 13a). This is the probability of a future basaltic dike intersecting the subsurface area of the potential repository. Furthermore, if a dike does intersect the repository, there is a 77% chance that one or more volcanoes would form along the dike within the repository footprint, with magma erupting through the repository. Both the intrusive and volcanic eruptive scenarios are considered in performance assessment because of the potential consequences of radionuclide release that could affect the critical group. The role of analogues in assessing the eruptive style of potential future volcanoes and their expected consequences is addressed in Section 14.3.

14.2.2 Seismicity

Yucca Mountain is located in the Basin and Range tectonic province, where earthquakes occur with some frequency. Geologic features of the site provide information on the region's past seismic activity, which is important in estimating the characteristics of future earthquakes. Based on these studies, the Yucca Mountain region has been rated as having low to moderate seismicity (CRWMS M&O 2000 [142321], Section 6.3.1). Seismic hazards are important to quantify as they could potentially affect the performance of a repository at Yucca Mountain. The seismic hazard at the site was assessed by a probabilistic seismic hazard analysis which produced results that allow assessment of the potential for ground shaking and fault rupture related to earthquakes (Wong and Stepp 1998 [103731]).

Extensive design experience gained through operating critical facilities, such as nuclear power plants, will be relied upon to ensure performance of the potential repository and its supporting facilities during and after an earthquake. During the postclosure period, the risks related to seismic activity will decrease because the waste will be deep underground where seismic waves are more attenuated. A surface seismometer and another seismometer at 245 m depth in the Exploratory Studies Facility (ESF) measured seismic waves from a 4.7 magnitude earthquake at Frenchman Flat, about 45 km (28 mi) east of Yucca Mountain (DOE 2001 [153849], Section 4.3.2.2). Recordings from this earthquake, shown in Figure 14-1, clearly indicate the decrease in amplitude of ground motions deep within the mountain. However, a strong earthquake could cause rockfalls in the emplacement drifts or alter the pathways followed by groundwater. Investigations of these potential consequences have concluded that it is highly unlikely that the consequences would be significant to repository performance (DOE 2001 [153849], Section 4.3.2.2). The role of analogues in building confidence in this conclusion is addressed in Section 14.4.

14.3 USE OF ANALOGUES IN VOLCANISM INVESTIGATIONS

Reasoning by analogy was used to debate the conceptual model for the probability of an igneous dike or dike system reaching the near surface without any portion of the system erupting. This is an important issue for volcanic hazard assessment of a potential repository at Yucca Mountain. The San Rafael volcanic field has been used as an analogue to argue that the probability of a separate intrusive event that does not erupt is 2 to 5 times higher than the probability of an eruptive event (NRC 1999 [151592]). However, the Analysis Model Report (AMR) *Characterize Framework for Igneous Activity at Yucca Mountain, Nevada* (CRWMS M&O 2000 [151551], Section 6.3.2.1) uses the Paiute Ridge igneous complex at the northeastern edge of the Nevada Test Site as an appropriate analogue to argue for a significantly lower rate for intrusions that do not result in eruption. Field observations at Paiute Ridge show that while some portions of individual dikes stagnated within approximately 100 m of the surface, other portions of the same dike did erupt. During the time period considered most significant by the panel of experts assembled for evaluating the volcanic hazard (the past 5 m.y., CRWMS M&O 1996, Figure 3-62), there is no known episode of dike intrusion to within a few hundred meters of the surface in the Yucca Mountain region that has not been accompanied by an extrusive event. Thus there is no evidence in the Yucca Mountain regional geologic record to suggest that dike intrusions without accompanying eruptions occur 2 to 5 times more frequently than eruptions (CRWMS M&O 2000 [151551], Section 6.3.2.1). An alternative interpretation of the San Rafael volcanic

field is also presented in the AMR *Characterize Framework for Igneous Activity at Yucca Mountain, Nevada* (CRWMS M&O 2000 [151551], Section 6.3.2.1), which supports an intrusion/extrusion ratio as being closer to 1. This interpretation assumes that it is likely that many individual intrusive/extrusive events are represented at San Rafael, where some portion of a dike system erupted during an event while other portions of the same dike did not erupt. This interpretation is more consistent with the geologic record of the Yucca Mountain region, as demonstrated at the Paiute Ridge analogue complex.

Analyses in the AMR *Characterize Eruptive Processes at Yucca Mountain, Nevada* (CRWMS M&O 2000 [142657]) assume that a plausible eruption during the postclosure performance period would be of the same character as Quaternary basaltic eruptions in the Yucca Mountain region. Eruptive styles and magmatic composition of the Lathrop Wells volcano, the most recent in the region, are emphasized as being the most characteristic. A new volcano would therefore contain some combination of scoria cones, spatter cones, and lava cones on the surface, and one or more dikes in the subsurface. Additional assumptions regarding the character of a future eruption focus on the use of data from a variety of analogue volcanoes and simplifications for a stylized plausible eruption. These include conduit diameter, dike width, the number of dikes associated with formation of a new volcano, magma chemistry, water content of magmas, gas composition, magma physical properties, ascent rate, fragmentation depth, mean particle size, and eruption duration, among others. This is an example of analogue information being used as direct parameter input into models, where the input consists of assumptions based on analogues.

The ASHPLUME computer code (Versions 1.4LV and 2.0) is used in estimation of the aerial density of an ash deposit. Ash-thickness data collected after the 1995 eruption of Cerro Negro, in Nicaragua, provided an opportunity to utilize the ASHPLUME code in simulating the eruption (CRWMS M&O 2000 [152998]). The application of this analogue information is discussed further in Section 15.

14.4 USE OF ANALOGUES IN BOUNDING EFFECTS OF SEISMICITY ON A GEOLOGIC REPOSITORY

Damage from ground shaking caused by an earthquake results largely from shear waves. Density contrasts along the path the shear waves follow from the earthquake source to the surface affect the amplitude of the waves. As the wave moves from dense rock at depth to less dense, more porous, and unconsolidated compressible material near the surface, the speed of the wave is reduced. With decreasing speed the kinetic energy of the wave is maintained by increasing amplitude, thus giving rise to increased shaking and intensity of damage. At the surface the amplitude of a shear wave will be about twice as large as at depth (Stevens 1977 [154501], p. 20). It follows that if the dimensions of an underground opening are considerably less than the wavelength of a shear wave, the shaking effects generated by the amplitude of motion will likewise be considerably less. The decrease in the effects of shear waves with increasing depth is comparable to the similar effect observed in ocean waves, which decrease in intensity and amplitude with the depth of water. A consequence of this is that the damage reported in shallow, near-surface tunnels is greater than that reported in deep mines (Pratt et al. 1978 [151817], p. 26).

There are numerous examples in the literature of underground structures withstanding damage from earthquakes that caused relatively greater damage at the ground surface (Eckel 1970 [157493]; Stevens 1977 [154501]; Sharma and Judd 1991 [154505]; Pratt et al. 1978 [151817]; Power et al. 1998 [157523]). Three earthquakes of recent decades, the Alaskan earthquake of March 28, 1964, the Tang-Shan, China, earthquake of July 28, 1976, and the Kobe, Japan, earthquake of January 16, 1995, clearly demonstrate the ability of underground structures to withstand the ground vibrations associated with severe seismic activity.

In the Alaskan earthquake, no significant damage was reported to underground facilities, including mines and tunnels, as a result of the earthquake, although some rocks were shaken loose in places (Eckel 1970 [157493], p. 27). Coal mines in the Matanuska Valley were undamaged, as was the railroad tunnel near Whittier, and the tunnel and penstocks at the Eklutna hydroelectric project. A small longitudinal crack in the concrete floor of the Chugach Electric Association tunnel between Cooper Lake and Kenai Lake is believed to have been caused by the earthquake. These reports of little or no damage to underground structures from the Alaskan earthquake are significant, because this earthquake was one of the largest (magnitude 8.5) to occur in this country, and the associated surface damage was extreme (Pratt et al. 1978 [151817], p. 32).

The July 28, 1976, earthquake in the heavily industrial city of Tang-Shan, China, had a magnitude of 7.8. Surface intensities at Tang-Shan were such that in the area where the strongest shaking occurred, 80% to 90% of the surface structures collapsed. However, for important engineered structures immediately below the surface, there was generally no serious damage regardless of the depth or size of the structure (Wang 1985 [151821], p. 741). The third example is the more recent Kobe, Japan, earthquake of January 16, 1995. Tunnels in the epicentral region of the Kobe earthquake (magnitude 6.9) experienced no major damage or even partial collapse for peak ground accelerations (PGAs) measured at the surface of ~0.6 g (Savino et al. 1999 [148612]).

A more site-specific, although smaller-magnitude, example was the Little Skull Mountain earthquake of June 29, 1992. This earthquake had a magnitude of 5.6 and occurred about 20 km from Yucca Mountain. Examination shortly after the earthquake of the interior of X-tunnel (125 m deep) in the epicentral region indicated no evidence of damage in the tunnel that could be associated with the earthquake (Savino et al. 1999 [148612]).

The understanding of the response of underground openings to seismic events has advanced greatly in the last 15 years. Sharma and Judd (1991 [154505], pp. 272–275) examined damage trends of underground facilities to seismic effects in an effort to aid future design of such facilities. They created a database consisting of 192 reported underground observations from 85 earthquakes throughout the world (Sharma and Judd 1991 [154505], p. 275). To examine the influence of seismic effects on underground openings, they used the measure of PGA that may be expected to occur at the surface directly above the underground location. The possibility of damage was examined as a function of (1) thickness of overburden, (2) predominant rock type, (3) type of ground support, (4) earthquake magnitude, and (5) epicentral distance of the earthquake.

On the basis of observations from this collection of data, Sharma and Judd (1991 [154505], p. 275) concluded that (1) damage incidence decreases with increasing overburden depth; (2) damage incidence is higher for unconsolidated colluvium than for more competent rocks; (3) internal tunnel support and lining systems appeared not to affect damage incidence; (4) damage increases with increasing earthquake magnitude and decreasing epicentral distance (increasing PGA); (5) no or minor damage can be expected for peak accelerations at the ground surface less than about 0.15 g. Data presented by Sharma and Judd (1991 [154505], Figure 7) indicate that damage to underground facilities at the depth for the potential repository is rare, even at accelerations of 0.4 g. These findings confirmed those of Stevens (1977 [154501], p. 36) and Pratt et al. (1978 [151817], p. 26), who suggested that the host material for an underground facility may be important in predicting the amount of damage caused by the shaking associated with earthquakes.

Although their observations contained 98 cases with no damage, Sharma and Judd (1991 [154505], p. 275) also acknowledge that their data set is biased towards occurrence of damage because "there must be literally hundreds of other instances where no damage occurred but observations were not documented" (Sharma and Judd (1991 [154505], p. 275). Two cases of moderate and heavy damage were reported in tunnels located at a depth of about 210 m near Santa Cruz, California, following the 1906 San Francisco earthquake. Based on the epicentral distance of 110 km, a PGA of 0.09 g was estimated. Generally, this PGA would be correlated with a "No damage" case; however, the epicentral distance on which the PGA estimate was based did not take into account the close proximity to the ruptured San Andreas Fault. Two other cases of damage also required further explanation. Damage reported for a mine in Idaho and the ERP Mine in the Witwatersrand, South Africa, at depths of 1,350 m and 3,000 m, respectively, was probably caused by rock-burst activity rather than a seismic event. This activity is usually pronounced in deep mines and generally can be recognized from the relatively high frequency content of the recorded accelerograms (Sharma and Judd 1991 [154505], p. 274). Stevens (1977 [154501], p. 33) quotes N.G.W. Cook of the South Africa Chamber of Mines as stating, "All the evidence indicates that earth tremors, rock bursts, and bumps arose in the Witwatersrand as a result of mining and have followed the pattern of mining in terms of frequency of incidents and epicentral position and focal depth".

Power et al. (1998 [157523]) collected extensive data on seismic ground-shaking-induced damage to bored tunnels, using more recent data from better instrumented earthquakes than was possible for Sharma and Judd (1991 [154505]). Power et al. (1998 [157523]) found that for ground motion with PGAs less than 0.2 g, there was little or no damage in tunnels, and for PGAs of 0.2–0.6 g, damage varied from slight to heavy (Power et al. 1998 [157523], Section 1.2). At even greater accelerations the damage only ranged from slight to moderate. For example, well-constructed tunnels near Kobe, Japan, experienced PGAs of about 0.6 g but suffered no major damage.

In addition to damage caused by ground vibration, underground tunnels can be damaged by fault displacement and by earthquake-induced ground failure, such as liquefaction or landslides at tunnel portals, which are not considered an issue at Yucca Mountain. In three instances of heavy damage from the 1923 Kanto, Japan, earthquake, observation of damage (with PGA equal to 0.25 g) may have resulted from landsliding. In the other two observed occurrences of heavy damage surveyed by Power et al. (1998 [157523]), tunnel collapse occurred in the shallow

portions of the tunnels. Damage to underground openings is inevitable only when the underground facility is displaced by a fault (Stevens 1977 [154501], p. 35). Carpenter and Chung (1986 [154504]) strongly recommend that faults with the potential for movement be avoided, which is consistent with design criteria for the potential repository at Yucca Mountain (BSC 2001 [155664], Section 1.2.2.1.5; McConnell and Lee 1994 [110957]).

The previous summary shows that tunnels withstand ground vibration well. However, tunnels in solid rock are susceptible to changes in hydrogeologic conditions and may be flooded as a consequence of ground shaking. Thus, although there may have been no apparent damage to the structure, there is a probability of increased fracture density in rocks surrounding the tunnels (Mumme 1991 [157494], p. 77). The potential for changes to the hydrogeologic system caused by fault displacement to affect radionuclide transport in the UZ at Yucca Mountain has been examined in the AMR, *Fault Displacement Effects on Transport in the Unsaturated Zone* (CRWMS M&O 2001 [151953]).

Even near the surface, damage from ground shaking may be slight if the rock is competent. For example, Mitchell Caverns, in the Providence Mountains of California, southwest of Las Vegas, sustained only minor damage in the October 16, 1999, Hector Mine earthquake (magnitude 7.1). The earthquake epicenter was only 30 miles (48 km) away. Damage was limited to a few stalactites being shaken from the ceiling at El Pakiva cave. At El Pakiva, the earthquake loosened some rocks from the face around and above its entrance (Figure 14-2), but the partial occlusion of its entrance by boulders was the result of a previous earthquake (Simmons 2002 [157544], p. 124). Another cave at Mitchell Caverns, Tecopa, experienced rockfall. The rockfall may be related to seismic events, but not to recent ones, because in some areas columns have been recemented by dripstone, and dripstone has begun to form on the ceiling from which the blocks fell. However, the area of cave floor covered by fallen blocks is much smaller than the total area of the cave, and fallen blocks have not obliterated the cavity opening.

Two final examples of the application of natural analogues to building confidence in the ability of a geologic repository at Yucca Mountain to withstand damage from ground vibration and faulting are the following. The AMR *Drift Degradation Analysis* (BSC 2001 [156304], Attachment VII) confirmed results of a rockfall model using information from natural analogues. The DRKBA code, used to model rockfall probabilities, involves a quasi-static method of reducing the joint-strength parameters to account for the seismic effect. This method was verified based on the test runs using the dynamic functions of the distinct element code UDEC. The comparisons between the results from the dynamic and quasi-static analyses showed a consistent prediction of block failure at the opening roof. The seismic effect on both the size and number of blocks in the rockfall model is relatively minor. This is consistent with information from natural analogues.

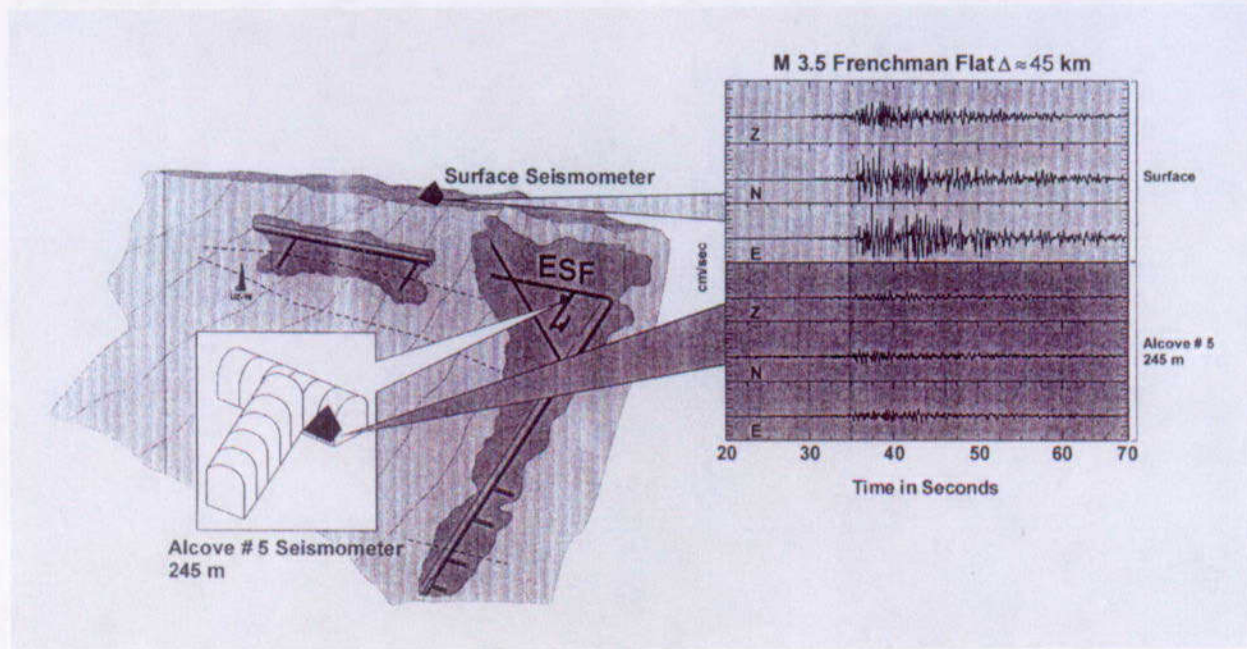
The AMR *Effects of Fault Displacement on Emplacement Drifts* (CRWMS M&O 2000 [151954]) included a literature survey on accommodating fault displacements encountered by underground structures such as buried oil and gas pipelines, which provide analogues for potential emplacement drift responses to fault offset.

The value of examining information on rockfall resulting from underground nuclear explosions (UNEs) was considered for this report. While an investigation on this topic may be fruitful, there

are significant differences between UNEs and earthquakes in terms of frequency content of the ground motion and the duration of shaking. These differences make the use of UNE results less relevant than results from earthquakes, although the effects of UNEs are better instrumented and documented than the effects of earthquakes.

14.5 SUMMARY AND CONCLUSIONS

Use of natural analogues is a major investigative tool in Yucca Mountain volcanism studies. Analogues have been used to assess the probability of dike eruption, plausible eruptive styles, eruptive parameters, and magma compositions, and have also been used to increase confidence in use of the ASHPLUME code for simulation of an eruption. Examples from observations of underground openings demonstrate that such openings are able to withstand ground shaking for even high PGAs. The ability to withstand ground shaking is increased by thickness of overburden, competence of material (rock versus colluvium), decreased earthquake magnitude, and increased distance of the opening from the earthquake epicenter. Underground openings may be damaged by landsliding or liquefaction associated with an earthquake, if the depth of the opening is relatively shallow. Underground openings are inevitably affected by fault displacement when the opening intersects a fault. Collateral damage by ground shaking can also be caused when ground shaking alters hydrogeologic conditions by increasing fracture density and permeability, and thereby increasing fracture flow to an underground opening. The bulk of evidence from analogue examples of underground openings, particularly in settings similar to Yucca Mountain, such as the Little Skull Mountain earthquake, demonstrates that damage to repository drifts by ground shaking during the postclosure period would be minimal or unlikely.



NOTE: The seismograms for the surface and underground are to the same vertical scale. M = magnitude; Δ = distance; Z = amplitude; N = N-S; E = E-W; ESF = Exploratory Studies Facility.

Source: Modified from Savino et al. 1999 [148612].

Figure 14-1. Recordings of Frenchman Flat Earthquake at the Ground Surface and the Thermal Test Alcove of the ESF



Source: Simmons 2002 [157578], SN-LBNL-SCI-108-V2, p. 9.

Figure 14-2. Entrance to Mitchell Caverns, El Pakiva Portal, Showing Fallen Blocks That Partially Occlude the Entrance

15. APPLICATION OF NATURAL ANALOGUES FOR THE YUCCA MOUNTAIN SITE CHARACTERIZATION PROJECT

15.1 INTRODUCTION

This section addresses the application of natural (including anthropogenic) analogues to geologic repository programs. Section 15.2 provides an overview of the applications for which natural analogues are suitable. Section 15.3 tells how natural analogues have been applied in geologic nuclear waste disposal programs worldwide. Section 15.4 reviews the application of natural analogues to past iterations of performance assessment (PA) and the supporting process models for Yucca Mountain. Section 15.5 identifies those model components, as stated by process modelers, that could benefit from confidence built through natural analogues. Section 15.6 categorizes the way natural analogue information has been used in this report. Section 15.7 presents a final summary and conclusions.

15.2 OVERVIEW

Figure 15-1 illustrates the flow of information from natural analogues and other site characterization data into PA models. The figure indicates that natural analogues provide both qualitative and quantitative information, as this report has demonstrated through many examples in the preceding sections. Stated in words, the stages or components in the development of a PA code (shown in Figure 15-1) are the following:

1. Construction of a conceptual model that describes the system and includes all of the important processes and their interactions
2. Translation of conceptual models into mathematical models and encoding those models in the form of a numerical code
3. Acquisition of input data for all the variable and constant parameter values included in the numerical code
4. Verification of the numerical correctness of the computer code
5. Validation of the code's applicability to the repository system in assessing its ability to predict future conditions.

The ways in which analogues can be or have been used to assist in 1, 3, 4, and 5 above are discussed below.

Model construction: In the stage of model construction, natural analogues can be used to tell the PA modeler:

- Which processes and process interactions to include
- Which processes are likely to be dominant and which are of secondary importance

- The spatial and temporal scales over which the model should perform
- Whether the basic premises of the model hold up under extrapolation to long time periods

Some of the analogues discussed in Sections 4, 6, 7, 9,10, 11, and 12 relate to identification of processes that are or may be included in models.

Data acquisition: Information derived from natural analogue studies is often semi-quantitative. For this reason it cannot often directly satisfy the parameter value requirements of a PA code. However, laboratory data have uncertainty related to the lack of similarity between the laboratory and repository systems. Therefore, a role for analogues in data acquisition is to provide a measure of validation for the laboratory data. Even though the analogue data may be imprecise, they can be used to give confidence in the reliability of the laboratory data. An example of this application was given in Section 4, describing the similarity between uraninite alteration phases produced in laboratory dissolution experiments and those uraninite alteration phases identified in rock samples at the Nopal I, Peña Blanca analogue site.

Model validation: Thermodynamic solubility and speciation codes and databases have been extensively applied in a number of natural analogue studies (e.g., Maqarin, Poços de Caldas, Koongarra). Natural analogues can help determine whether the solubility-controlling mineral species and complexes in solution (generally specified by hydrochemical databases or from theoretical or laboratory experiments) are appropriate to the site-specific conditions being modeled, and whether or not mineral phases and/or ionic species in solution indicate chemical equilibrium has been achieved or whether the system is controlled by kinetics.

A subcategory of modeling studies is database evaluation. One application of natural analogues in this category is the evaluation of geochemical models and numerical tools used in describing the predicted migration of radionuclides in a repository system. Blind predictive modeling comparisons are a means of evaluating geochemical databases. For instance, Bruno et al. (2001 [157484]) reviewed and compared the results obtained from the blind prediction modeling exercise carried out for seven natural analogue studies relevant to European repository concepts: Oman; Poços de Caldas, Brazil; Cigar Lake, Canada; Maqarin, Jordan; El Berrocal, Spain; Oklo, Gabon; and Palmottu, Finland. The blind predictive model exercise (Bruno et al. 2001 [157484]) was able to improve conceptual and numerical models to identify relevant radionuclides to major component phases in the rock-water systems of interest. The group achieved a consensus concerning the most appropriate methodology for approaching solubility-limited calculations and identified the main requirements for acquiring improved site characterization data to describe radionuclide mobility.

Tangible illustrations: Natural analogues also have an important role, beyond their application to PA, in providing illustrative information to a broad range of audiences, including the general public. Natural analogues, or comparisons with natural systems, are frequently mentioned as important components of the process of evaluation and acceptance of disposal concepts. In quoting the IAEA (1999 [157485]), Miller et al. (2000 [156684], Section 6.1) stated, "Among all levels of reviewer, from technical peer review panels to nontechnical audiences, there is a clear belief that PAs are only credible if shown to have strong natural parallels." Recognition of the important processes and events that control the repository behavior can be demonstrated from

illustrative geological analogues. Natural analogue assist in the public understanding of the timescales applicable to radioactive decay. These real world examples are important because the extended time periods of interest to disposal are generally longer than those in our normal range of experience.

15.3 PERFORMANCE ASSESSMENT APPLICATIONS OF ANALOGUES IN GEOLOGIC DISPOSAL PROGRAMS WORLDWIDE

Several reviews have examined the level of direct and acknowledged use of natural analogues in published PA documents of geologic repository programs worldwide (e.g., McKinley and Alexander 1996 [157486]; IAEA 1999 [157485]). Results of these reviews indicated that very few total system PA documents provided detailed discussion of how analogues were used to support specific aspects of the assessments, and some PA reports did not discuss how natural analogues support geological disposal in even a general way.

An indirect use of analogues in PA in some programs is in the development of scenarios, where identification of features, events, and processes (FEPs) of importance to repository evolution are required (Chapman et al. 1995 [100970]). The role of analogue information in this case is to provide supplemental evidence to support the inclusion or exclusion of different FEPs in scenarios to be analyzed for PA. An example of this application of analogues is the scenario case for criticality in a waste repository. This scenario was screened out using, in part, understanding of processes that occurred at Oklo (see Section 4).

Miller et al. (2000 [156684], Section 6.1), referring to IAEA 1999 [157845], summarized the use of analogues for model development, data provision, and model validation in ten PAs over the past two decades. These included KBS-3 (Sweden, 1983); Projekt Gewähr (Switzerland, 1985); SKB-91 (Sweden, 1991); TVO (Finland, 1991); AECL EIS (Canada, 1994); Kristallin-I (Switzerland, 1993); NRC IPA (USA, 1995); TILA-99 (Finland, 1999); SR-97 (Sweden, 1999); and SFR (Sweden, 1999). All but one of these PAs used analogues in conceptual model development or scenario development. All of the PAs used data from analogues, either as bounding conditions or as direct parameter values. Seven of the ten PAs used analogues for blind predictive modeling or for the evaluation of models and databases as part of model validation. The NRC, for instance, used natural analogues in the following ways:

- In scenario development for volcanism, as an alternative source-term conceptual model using Peña Blanca data (Murphy and Codell 1999 [149529])
- To establish relative importance of microfractures and matrix transport at Peña Blanca, Mexico
- As backup for vapor-phase transport at the Valles Caldera, New Mexico
- To identify secondary phases for long-term release at Peña Blanca
- For model testing for elemental transport in unsaturated media at Akrotiri, Greece (Murphy 2000 [157487]).

Miller et al. (2000 [156684], Table 6.1.1) noted that few of the analogue applications were explicitly mentioned in the top-level documents associated with these PAs. The lack of acknowledgment of these applications of analogues by PAs is evident from a disconnect between the examples of uses shown in the IAEA (1999 [157485]) report and the applications noted in the report's conclusions. Thus it appears that the role of natural analogues in providing a general conceptual basis for the geological disposal of radioactive waste and for specific waste isolation mechanisms is largely unacknowledged. There are only a few clear examples of parameter values being provided by natural analogues that may be directly input to an assessment model, such as measured matrix diffusion and metal corrosion rates. A semi-quantitative use of natural analogues has been to provide bounding limits to the ranges of parameter values obtained from laboratory studies. The most valuable quantitative role of natural analogues, which cannot be replicated in laboratory systems, is to provide bounding estimates for validation of PA models. So far, this has only been seriously attempted for equilibrium geochemical modeling (e.g., at Poços de Caldas, Oman, Maqarin, and El Berrocal).

15.4 PREVIOUS YMP INCORPORATION OF NATURAL ANALOGUES

Process modelers, as users of analogue information, can and have played an important role in determining how analogues can best be used to support PA and design groups in reducing uncertainties in the long-term behavior of natural and engineered systems.

In the past, the YMP has used analogues for testing and building confidence in conceptual and numerical process models in a number of ways:

- Yucca Mountain as a self analogue: Mineral alteration zones that formed during cooling of Timber Mountain ash flow tuffs are the same as those expected to form under the thermal conditions predicted by numerical codes (Bish and Aronson 1993 [100006]).
- Thermochemical data: Data from the Wairakai, New Zealand, geothermal field were used to build confidence in thermodynamic parameters for silica minerals in databases used in geochemical modeling (Carroll et al. 1995 [109627]).
- Spent fuel alteration parageneses: Mineral phases determined in laboratory experiments were compared to those of Nopal I, at Peña Blanca (Figure 4-1). The results of these studies (summarized in Section 4) have increased the confidence in models describing spent-fuel alteration.
- Saturated zone transport: Scoping calculations were conducted for the Peña Blanca site using the same numerical model that was used to assess total system performance of the potential Yucca Mountain repository. The model attempted to predict the transport of ^{99}Tc , which is expected to be a conservative ion that would be released from the waste inventory. Results of the modeling indicated that both ^{99}Tc and some forms of uranium may be detected in groundwater close to the Nopal I mine at Peña Blanca (CRWMS M&O 2000 [153246], Appendix C, Figure C-12). The scoping predictions were sensitive to the surface area assumed for the inventory of leachable mineral species, because a reduction of mineral surface area led to a reduction in both uranium and ^{99}Tc .

concentrations (CRWMS M&O 2000 [153246], Appendix C). The scoping study predictions differ from analyses of groundwater samples collected in the 1980s from a monitoring well 1,300 m downgradient from the Nopal I mine, which detected very low concentrations of uranium. To corroborate the model results for uranium and possibly technetium, the scoping simulations could be rerun using additional data from analyses of water samples collected from wells being drilled at and immediately downgradient from the Nopal I ore deposit (see Section 10.4).

- Verification of models describing volcanism: Immediately after a 1995 volcanic eruption at Cerro Negro, an active basaltic cinder cone in Nicaragua, the thickness of volcanic ash deposited during the eruption was measured. The ash thickness data provided an opportunity to use the ASHPLUME code (CRWMS M&O 1999 [132547]) to simulate the eruption. The goal was to compare calculated ash deposition predicted using the ASHPLUME code to the ash thickness recorded in an actual ashfall event from a small-volume basaltic volcano. Cerro Negro is analogous in size and morphology to a volcanic feature that could form as the result of a volcanic eruption in the vicinity of Yucca Mountain, although the intra-continental arc magmatism that forms the tectonic setting for Cerro Negro is different from the Basin-and-Range style tectonics of the Yucca Mountain area. Two versions of the ASHPLUME code that employ a two-dimensional diffusion model were used. The results of both versions compared well with the observed data for distances from the volcanic event greater than 10 km (CRWMS M&O 2000 [153246], Appendix C, Figure C-1). For distances less than 10 km, ASHPLUME results calculate ash thickness values greater than the observed data, possibly because ASHPLUME assumes a constant wind speed and direction for a given simulation, whereas the actual situation reflected a shift in wind direction, and possibly velocity, during the eruption. Nevertheless, the results in general showed that the ASHPLUME model can reasonably predict the ashfall distribution of a basaltic cinder cone similar to Cerro Negro. This result increases the confidence in ashfall calculations that could be used to simulate possible ash-producing eruptions either near or through a repository at Yucca Mountain.

Analogues were included in discussions of multiple lines of evidence in the *FY 01 Supplemental Science and Performance Analyses, Volume 1: Scientific Bases and Analyses* (BSC 2001 [155950]). To a large degree, these analogues have been referenced in this report in Sections 4, 6, 7, 8, 9, 10, 11, 12, 13, and 14. Analogues have also been used to provide multiple lines of evidence in support of both analysis and model reports (AMRs); in screening arguments for inclusion or exclusion of FEPs in total system PAs (TSPAs); in the quantification of uncertainties (BSC 2001 [155950]); and in expert elicitations such as *Probabilistic Volcanic Hazard Analysis for Yucca Mountain, Nevada* (CRWMS M&O 1996 [100116]); *Probabilistic Seismic Hazard Analyses for Fault Displacement and Vibratory Ground Motion at Yucca Mountain, Nevada* (USGS 1998 [100354]); and *An International Peer Review of the Biosphere Modelling Programme of the US Department of Energy's Yucca Mountain Site Characterization Project, Report of the IAEA International Review Team* (IAEA 2001 [155188]).

15.5 YMP IDENTIFIED NEEDS

Areas identified for the TSPA-VA in which analogue studies might contribute to evaluating of and building confidence in PA models include:

- Seepage threshold and the fraction of waste packages contacted by seeps (including seepage enhanced by thermally induced drift collapse)
- Alteration of hydrologic properties by mineral precipitation or dissolution
- Sorption onto fractures
- The role of colloid filtration in reducing radionuclide migration
- Alloy 22 corrosion
- Np solubility
- Saturated zone (SZ) dilution.

PA requirements for natural analogues were also considered for TSPA-SR and TSPA-LA. A meeting was held in January 2001 to integrate PA needs for building confidence in process models, including areas where natural analogues could contribute. This report includes examples of natural analogue contributions to the stated needs found in performance assessment studies.

15.6 APPLICATIONS FROM THIS REPORT

Table 15.1 is a compilation of the ways in which analogues have been used in this report. The analogues are listed by chapter and are categorized as to their use in building conceptual models or understanding of processes, development of data parameters and their use in TSPA, or use for model validation. It is evident that the majority of uses of analogues for YMP has been in the understanding of which processes to model and how to incorporate them into PA. Less frequent has been their use in model validation, and even less frequent is their use directly in PA. The categorization on this table should not be surprising because it corresponds to the frequency of application of analogues to these steps in TSPA in the international community, as stated in Section 15.3 and in IAEA (1999 [157485], Section 6).

15.7 SUMMARY AND CONCLUSIONS

This section recapitulates the most important points that were summarized at the end of each preceding section, along with suggestions for areas where analogues could increase needed confidence in process models. Because no new material is introduced in this section, the references to these conclusions are not included. The reader should refer to the section that provides the source of these summary points, or conclusions, or to the Document Input Reference System (DIRS).

15.7.1 Drift Stability (Section 3)

The ability of underground openings to remain open and stable under ambient conditions depends on a number of variables, including: (1) rock strength; (2) the size, shape, and orientation of the opening; (3) orientation, length, and frequency of fracturing; and (4) effectiveness of ground support. Radiometric dating of cave floor minerals at Carlsbad Caverns and Lechuguilla Cave indicates that natural openings larger than those proposed for repository drifts at Yucca Mountain have remained stable and open for millions of years. Collapse of the roof of an opening tends to occur where the fracture density is high and the overburden is thin, as is the case with some lava tubes. Independent factors that contribute to the size of a rockfall block are fracture spacing, rock type, rock texture, and the size and shape of the opening. Paleolithic flint mines (~4,000 to 3,000 BC), Roman mines and aqueducts, and other anthropogenic examples demonstrate that man-made underground openings can also exist for thousands of years.

15.7.2 Waste Form Degradation (Section 4)

The reaction path of alteration of spent nuclear fuel at Yucca Mountain will be similar to that of geologically young, Pb-free uraninite, with schoepite and becquerelite forming as intermediate products, followed by uranyl silicates. The uraninite and its alteration products found at the Nopal I uranium deposit at Peña Blanca have these characteristics. Therefore, the uranium alteration paragenetic sequence at the Nopal I uranium deposit at Peña Blanca is a good analogue for the alteration of uranium oxide spent fuel.

Secondary mineral formation was responsible for incorporating uranium in stable mineral phases at Shinkolobwe, Zaire, where 50 secondary uranium-bearing phases could be identified. Because of its great age (1,800 Ma), radiogenic lead-bearing phases played a role in sequestering uranium. At Okélobondo, Gabon, and Shinkolobwe, other secondary phases, particularly (U,Zr) silicates, formed stable phases.

The concentrations of fission products can be used as tracers in rock and groundwater surrounding uraninite and provide a satisfactory approach to estimating natural dissolution rates. When this approach was evaluated at Cigar Lake, Canada and Koongarra, Australia under reducing and oxidizing conditions, respectively, the dissolution rate at Koongarra was found to be more rapid. Although use of the fission product tracer method has not been reported for Oklo, other lines of evidence indicate that dissolution has been slight at Oklo over the past approximately 2 billion years. Whether or not deep oxidizing waters at Okélobondo have increased the dissolution of uraninite and created an oxidized suite of minerals is a subject that could be evaluated.

Under radiolysis conditions occurring at the time of reactor criticality at Oklo, only several percent of uranium was estimated to have been mobilized for transport from its original site, which experienced far more extreme conditions than those anticipated at Yucca Mountain. Likewise at Okélobondo, radiolysis effects at the time that the natural reactor was active appear confined to rare earth element migration from the core to the rim of minerals containing these elements.

Based on analyses of conditions that occurred at Oklo, it was shown that criticality of spent fuel either within waste packages or by reconcentration of uranium outside of the waste package has a very low likelihood, because the probability of certain processes required to achieve critical conditions occurring simultaneously or sequentially is extremely small and certain required conditions are mutually exclusive.

Although natural glasses are somewhat different in composition from borosilicate nuclear waste glass, studies of natural glass alteration indicate that glass waste forms will be stable in a repository environment at Yucca Mountain. In both natural and borosilicate glass, higher stability is favored by higher silica and alumina content and by lower alkali and water content. However, analogue studies have not considered radiation effects on glass over long time periods and thus cannot be used to confirm experimental results showing that radiation has little effect on waste glass stability.

15.7.3 Waste Package Degradation (Section 6)

The analogues to common metals presented in Section 6 serve mainly to demonstrate that under ambient to slightly elevated temperatures, these metals will be stable for thousands of years, even under oxidizing conditions. The survival of metal archaeological artifacts over prolonged periods of time is related to the corrosion-resistant properties of metals and metal alloys, the development of protective passive film coatings with the onset of corrosion, and the location of artifacts in arid to semi-arid environments. Such features have been used in the selection of materials and design configuration to enhance the durability of waste packages at Yucca Mountain.

The survival of the naturally occurring ordered Ni-Fe alloy in josephinite for millions of years, with only relatively minor amounts of surface oxidation, indicates that this material is highly resistant to oxidation and other forms of corrosion that occur in its geologic environment. While the composition of this metal differs from Alloy 22 (in that it does not contain Cr, Mo, or W), it does provide evidence that a similar alloy can remain passive over prolonged periods of time under similar conditions.

The potential instability of chromium-bearing materials is illustrated by the observed natural release of chromium from chromite in the Sierra de Guanajuato ultramafic rocks under ambient conditions. Corrosion appears to be concentrated along exsolution rims, analogous to structural defects on metal surfaces. However, although the chromite has undergone some alteration, it has survived for over 140 million years.

15.7.4 Engineered Barrier System Components (Section 7)

The highly corrosion-resistant nature of titanium has been demonstrated by long-term experiments conducted on a range of metal alloys in wells at the Salton Sea geothermal field, California. This anthropogenic example supports the selection of titanium alloys for the construction of a corrosion-resistant drip shield for the Engineered Barrier System (EBS).

Although the proposed devitrified welded tuff for the invert ballast does not have high concentrations of zeolite and clay minerals, the high surface area of crushed tuff will retard radionuclide transport through sorption. One example of absorption of actinides in a gravel bed

at Los Alamos, New Mexico provides qualitative evidence of retardation at the contact between an invert-like material and underlying bedrock.

Because the use of cementitious material in the EBS and its environs is restricted to grout for securing rock bolts in the emplacement drifts, hyperalkaline conditions are not expected to develop at Yucca Mountain. However, through reactive-transport modeling of the Maqarin site, it has now been demonstrated that a model can reproduce the same suite of cement minerals, hyperalkaline water compositions, and pH that were found in the field. This result builds confidence in use of such a model for analogous conditions at other sites.

The Poços de Caldas analogue illustrated that iron-bearing colloids may retard the transport of uranium and other spent-fuel components by forming colloids that are then filtrated from suspension at short distances. Degradation of steel structural elements in the EBS could conceivably contribute to this process.

15.7.5 Seepage (Section 8)

An important variable for preservation in underground openings is relative humidity. If relative humidity in the emplacement drift is kept below 100% by ventilation, then seepage of liquid water would be reduced or completely suppressed. Most caves are close to, but below 100% humidity. Thus the amount of seepage in caves found in unsaturated environments would be expected to be low. This would also be true at Yucca Mountain while ventilation is maintained.

The findings in Section 8 support the hypothesis that most of the infiltrating water in the unsaturated zone (UZ) is diverted around underground openings and does not become seepage. The analogues show that this is true even for areas with much greater precipitation rates than that at Yucca Mountain. Although examples exist where large amounts of seepage can be observed (e.g., the Mission Tunnel and Mitchell Caverns), and cave minerals formed by water are common in unsaturated environments, these hydrogeologic settings are significantly different from that at Yucca Mountain, and thus these are not appropriate analogues. However, for all of the analogues that show some seepage, at least some of the seepage that enters underground openings does not drip, but rather flows down the walls. In the few instances where dripping has been noted in settings that are analogous to Yucca Mountain, the drips can be attributed to asperities in the surface of the roof and ceiling of the opening. Whether water flows on walls or drips depends on conditions affecting drop formation and drop detachment (e.g. surface tension, roughness angle, saturation). Thus, although most water would flow around emplacement drifts at Yucca Mountain, the small amount of seepage that does occur would primarily flow down tunnel walls. In the few instances where dripping may occur, it would be expected to occur at asperities also.

15.7.6 UZ Flow and Transport (Sections 9 and 10)

Hydrographs of ponded water and ⁷⁵Se breakthrough curves measured during the LPIT test conducted at the Idaho National Engineering and Environmental Laboratory (INEEL) were analyzed to determine parameters controlling unsaturated flow and transport. Analysis of these data involved building a numerical model using TOUGH2 in a dual-permeability modeling approach that has been extensively used to simulate flow and transport at Yucca Mountain. The

basalt hydrologic properties showed significantly greater variability than the B-C sediment layer interbed properties. This implies that the field-scale heterogeneity limits the volume to which the spatially averaged basalt parameters could be attributed relative to the B-C sediment layer interbed parameters. This may in part result from the fractured-porous dual-continuum nature of the basalt in comparison to the porous single-continuum nature of the B-C sediment layer interbed.

The transport model calculations predicted retardation factors for neptunium and uranium that are orders of magnitude higher than retardation factors for the other radionuclides at the Radioactive Waste Management Complex (RWMC). This result would indicate that very little movement of neptunium and uranium should be observed. But detection of these radionuclides at depth was inconsistent with their predicted high retardation. Radionuclide transport in the surficial sediment zone at the RWMC could be interpreted in a number of ways. One is that lateral flow occurred, sweeping out part of the radionuclide plume. Another possibility is that a sudden surge of fluid caused by a flooding event released a pulse of radionuclides that propagated downward quickly, such that the peak lies at a greater depth than that at which the data were collected. The UZ Flow and Transport Model at Yucca Mountain considers a range of infiltration rates that are then used to bound the range of percolation flux. Because the Paintbrush nonwelded unit (PTn) at Yucca Mountain has a damping effect on downward flow to the Topopah Spring welded unit (TSw), and a similar damping effect has not been observed in the sedimentary interbeds at the RWMC, it is unlikely that the enhanced transport scenario proposed in the INEEL modeling study would occur at Yucca Mountain.

It is estimated that the transit time for the seep water that infiltrated into the Nopal I Level +00 adit 8 m below surface is about 6–29 days, and for the perched water at 10.7 m depth in an old borehole, the transit time is about 0.4–0.5 years. Although the water transit time in the UZ is quite short, significant dissolution of uranium may have occurred in a low-water flux, high-uranium concentration setting near the Nopal I uranium deposit. The uranium dissolution rates at Nopal I are about three times higher during the dry season than those in the wet season, possibly suggesting a favorable physiochemical condition (e.g., increased oxygenation) for uranium dissolution during dry periods. The low humidity during dry seasons may have also enhanced evaporation, causing higher uranium concentrations in the waters sampled. If analyses from future sampling campaigns confirm that transit time is short in the UZ at Nopal I, then the implications would need to be considered for the similar low-water flux environment at Yucca Mountain.

15.7.7 Coupled Processes (Section 11)

Geothermal systems illustrate a variety of thermal-hydrologic-chemical (THC) processes that are relevant to Yucca Mountain. Yellowstone and other geothermal systems in welded ash flow tuffs or other low-permeability rocks indicate that fluid flow is controlled by interconnected fractures. Alteration in low-permeability rocks is typically focused along fracture flow pathways. Only a small portion of the fracture volume needs to be sealed by precipitated minerals to retard fluid flow effectively. The main minerals predicted to precipitate in the near field of the potential Yucca Mountain repository are amorphous silica and calcite, which are also commonly found as sealing minerals in geothermal systems.

Sealing in geothermal fields can occur over a relatively short time frame (days to years). The unsaturated conditions, lower temperatures, and much lower fluid-flow rates predicted for the Yucca Mountain system, in comparison to geothermal systems, should result in less extensive water-rock interaction than is observed in geothermal systems. Fracturing and sealing occur episodically in geothermal systems. Most mineralization at Yucca Mountain is predicted to occur soon after waste emplacement (1,000 to 2,000 years), when temperatures would reach boiling (for the higher-temperature operating mode) above the emplacement drifts.

As shown in Section 11.3, THC processes are expected to have a much smaller effect on hydrogeological properties at Yucca Mountain than what is observed at Yellowstone. However, development of a heat pipe above emplacement drifts at Yucca Mountain under a higher-temperature operating mode could lead to increased chemical reaction and transport in the near field. Reflux and boiling of silica-bearing fluids within the near field at Yucca Mountain could cause fracture plugging, thus changing fluid flow paths. Geochemical modeling of fluid compositions has been used to successfully predict observed alteration mineral assemblages at Yellowstone. THC simulations conducted to date for the potential Yucca Mountain repository suggest that only small reductions in fracture porosity (1–3%) and permeability (< 1 order of magnitude) will occur in the near field as a result of amorphous silica and calcite precipitation. Changes in permeability, porosity, and sorptive capacity are expected to be relatively minor at the mountain scale, where thermal perturbations will be reduced. This THC result applies to both the higher and lower temperature (sub-boiling) operating modes. These predicted changes in hydrogeological properties should not significantly affect repository performance.

At the Paiute Ridge intrusive complex (Section 11.4), the Papoose Lake Sill intruded into Rainier Mesa Tuff, and the resulting hydrothermal effects were characterized by low-temperature alteration of glass to clinoptilolite and opal, similar to the alteration assemblage present at Yucca Mountain. Hydrothermal alteration was confined to a narrow zone close to the sill-host rock contact. The pervasive opal veins and associated secondary minerals (e.g., clinoptilolite, calcite, cristobalite, etc.) appear to have reduced matrix or fracture permeability in the immediate vicinity of the basaltic intrusion.

Preliminary results of a one-dimensional THC dual-continuum model of the interaction of country rock with heat released from an intrusive complex emplaced above the water table demonstrated the possibility of forming opal-filled veins with the source of silica derived from the matrix of the host rock. However, because of the irregularities caused by kinetic barrier effects associated with reaction of glass, it is important to compare and contrast a number of different sites to be able to derive general conclusions regarding mineral alteration.

Although rock type, hydrogeology, and design configurations differ from those at Yucca Mountain, the closest thermal-hydrologic-mechanical (THM) analogue identified so far is the K-26 site at Krasnoyarsk, which is particularly relevant to lower-temperature design scenarios. Although the 40-year record of experiments should be interpreted cautiously with respect to extrapolation to long time periods, THM effects such as drift convergence might be in the same range of magnitude (on the order of a few mm) as that at Krasnoyarsk for the preclosure period.

15.7.8 Saturated Zone Transport (Section 12)

Only a few of the Uranium Mill Tailing Recovery Act (UMTRA) sites are potentially useful in the evaluation of radionuclide transport in the alluvial portion of the Yucca Mountain flow system. The conclusions derived from an analysis of the Gunnison site are: (1) a fraction of the uranium originating at the site is transported in the alluvial aquifer at a rate similar to the rate at which a conservative constituent is transported; and (2) there is little evidence for lateral dispersion of contaminants in the downgradient direction. For the New Rifle site, the main conclusions are: (1) dilution is a significant process in the downgradient direction; and (2) uranium is transported at almost the same rate as conservative constituents. The conclusions regarding uranium transport distances relative to conservative constituents must be tempered by uncertainties regarding the potential presence of unidentified complexing agents.

Although several natural analogue studies have demonstrated the effect of sorption and precipitation processes on fracture surfaces, none has been able to distinguish clearly between these processes or to provide quantitative data on retardation with respect to transport of trace elements in natural waters. However, these studies do highlight which phases are most active and provide useful information on the effect of interaction between solutes and the rock surface.

In most studies of natural systems, a proportion of the total uranium, thorium, and rare earth elements in the groundwater was associated with colloids. Colloids can serve as sorbers of radionuclides, and may be agents either of retardation (Section 7 and Section 15.7.4) or of fast transport (Section 12). Unambiguous evidence from natural systems indicating colloidal transport over kilometer-scale distances is limited to a few reports. Observations from such places as Los Alamos and the Nevada Test Site lend support to the concept that radionuclide transport in the saturated zone (SZ) can be facilitated by colloids, but so far no natural analogue studies have been able to quantify the importance of this process.

15.7.9 Biosphere (Section 13)

The Chernobyl data on hot-particle dispersal and dust transport showed that radionuclides attach to dust particles and move as combined particles. Aspects of models of atmospheric contaminant dispersal, radionuclide fallout, radionuclide resuspension, and particle size distributions may be relevant to constraining a model for radionuclide resuspension resulting from a volcanic eruption through a potential Yucca Mountain repository.

The use of physical values of the half-life of radionuclides gives conservative estimates of radionuclide removal from soils in the Yucca Mountain biosphere model. The increase in the concentration of radionuclides in soils during irrigation in the southern Ukraine, where environmental conditions are more similar to those at Yucca Mountain than are conditions at Chernobyl, confirms the concept of a radionuclide buildup factor used in the Yucca Mountain biosphere conceptual model.

Results of the Chernobyl literature survey suggest that soil type influences the ecological half-life of radionuclides in the biosphere, both in regard to soil bioaccumulation factors, and advective and diffusive transport properties that limit radionuclide transfer to plant roots. With respect to rural populations, agricultural methods including irrigation, tillage, and types of crops

play an important role in resuspension of radionuclides. Resuspended material is likely to increase the contamination of plant surfaces. Resuspended radionuclides would increase the inhalation dose for agricultural workers, which would be particularly significant for plutonium.

For potential groundwater contamination pathways at Yucca Mountain, radionuclide-contaminated water, which is used as the source of drinking water, irrigation, animal watering, and for domestic applications, is expected to increase the likelihood of ingestion uptake of radionuclides by humans. Chernobyl data showed that the ingestion pathway constitutes a small part of the total radiation dose, as the external pathway is predominant within the Chernobyl Exclusion Zone. Chernobyl data on the atmospheric distribution of contaminants, their fallout, and redistribution in soils and plants may be considered an anthropogenic analogue for the potential release of radionuclides caused by a volcanic eruption at Yucca Mountain, accompanied by atmospheric dispersal of contaminants into the environment through ash fallout on the land surface.

15.7.10 Volcanism and Seismic Effects on Drifts (Section 14)

Use of natural analogues is a major investigative tool in Yucca Mountain volcanism studies. Analogues have been used to assess the probability of dike eruption, plausible eruptive styles, eruptive parameters, and magma compositions, and have also been used to increase confidence in use of the ASHPLUME code for simulation of an eruption. For seismic effects, examples from observations of underground openings demonstrate that such openings are able to withstand ground shaking for a peak ground acceleration as high as 0.4 g. The ability to withstand ground shaking is increased by thickness of overburden, competence of material (i.e., indurated and consolidated rock versus colluvium), decreased earthquake magnitude, and increased distance of the opening from the earthquake epicenter. The bulk of evidence from analogue examples of underground openings, particularly in settings similar to Yucca Mountain (such as the Little Skull Mountain earthquake), demonstrates that damage to repository drifts by ground shaking during the postclosure period would be minimal or unlikely.

15.7.11 Remaining Areas for Increased Process Understanding through Analogue Studies

The analogue examples and studies presented in this report provide varying degrees of confidence in the processes they are intended to support. The investigation of these analogues has helped to indicate the directions along which further analogue studies can best be focused to address processes that are not fully understood. Key areas where analogues may assist in building more confident assessments of processes are the following:

- **Irreversible Sorption**: PA currently makes the conservative assumption that sorption is reversible because no useful data exist that show it to be irreversible. If analogues could demonstrate convincingly the conditions under which sorption could be irreversible, they would contribute greatly to the realism of models.
- **Drift Shadow Zone**: The presence of a drift shadow zone is best tested through analogue sites that have remained undisturbed over several decades. Suggested sites are discussed in Section 9.

- Plume Dispersion: Following the UMTRA study, modeling of different types of plumes in alluvium could build confidence in the way plume dispersion is modeled for YMP TSPA. Examples could be found with toxic spills or natural analogues such as Koongarra.
- Geosphere/Biosphere Interface: Radionuclide behavior at the geosphere/biosphere interface could be investigated by natural analogue studies on the migration of radionuclides released from spills, leaks, and underground bomb tests and accidents. Some sites in Russia may yield these types of data.
- Colloids: Analogue studies suggest that colloids provide an inefficient mechanism for transport because of low populations, limited radionuclide uptake, and filtration by the rock. However, to conclude that colloids are an unimportant factor for repository safety would require information from larger-scale natural studies in relevant geological environments, which would allow study of the efficacy of buffering reactions for Eh and pH and evidence for long-distance (km-scale) transport in relevant geologic formations.
- Transport in Unsaturated Ash Flow Tuffs: Peña Blanca is probably the closest overall analogue with conditions similar to Yucca Mountain. Nopal I is a natural environment where groundwater chemistry is somewhat analogous to groundwaters in the Yucca Mountain system, and they contain elevated concentrations of radionuclides and other trace elements from a known source. Nopal I also displays discrete zones in fractured rocks intersected by potentially identifiable preferential groundwater flow paths. Such flow paths would allow definition of a source region and transport pathway, as well as a study of sorption processes on fracture surface minerals.

Table 15-1. Natural Analogues in This Report and Their Potential Applications to Performance Assessment

Section in Natural Analogue Report	Conceptual Model Development (Applied Processes from Natural Analogues)	Use of Specific Parameters in Yucca Mountain TSPA Model	Use for Model Validation of Yucca Mountain Characterization
3.2			Dimensions of caves and underground openings that have stood open for thousands of years
3.3			Man-made openings have stood open for thousands of years (oldest 4000 B.C.)
3.5	Variables that determine structural stability of underground openings		
4.2, 4.4			Nopal I validated spent fuel dissolution experiments where U-silicates are long-term solubility-limiting phases
4.3	Retention of fission products at Oklo related to partitioning into uraninite		
4.4	Importance of secondary phases at Shinkolobwe and Okélobondo in retaining U		
4.6			Chemical and physical conditions required to reach criticality at Oklo used to estimate amount of spent fuel needed to create critical conditions at a repository
4.7			Qualitative validation that natural glass alteration studies indicate nuclear waste glass will be stable in repository environment
6.2	Enhanced preservation of objects stored in unsaturated conditions, as observed in Pintwater cave (NV)		
6.2	Vapor condensation resulting in corrosion, as observed in Altamira cave (Spain)		
6.2	Effects of hypersaline fluids on waste package materials, as observed in corrosion behavior of different metal compositions at Salton Sea (CA) geothermal field	Evaporation experiments conducted to determine evolution of Yucca Mountain water compositions and corresponding mineral precipitate	

Table 15-1. Natural Analogues in This Report and Their Potential Applications to Performance Assessment (cont.)

Section in Natural Analogue Report	Conceptual Model Development (Applied Processes from Natural Analogues)	Use of Specific Parameters in Yucca Mountain TSPA Model	Use for Model Validation of Yucca Mountain Characterization
6.2	Formation of protective passive film around metals, as observed in Delhi iron pillar (India)		
6.2	Long-term stability of Ni-Fe metals, as evidenced by occurrence of josephinite in 150 million year old ultramafic rocks (OR)		
7.2	Effects of hypersaline fluids on titanium, as observed in corrosion behavior of titanium alloys at Salton Sea (CA) geothermal field		
7.2	Effects of zeolites and clay minerals on ion exchange and sorption of radionuclides, as observed in tufts at Yucca Mountain and Los Alamos, NM		
7.3	Development of hyperalkaline plumes from cementitious materials, as observed at Maqarin (Jordan)		Multicomponent reactive transport model used to compare simulated and observed fluid chemistry and rock alteration mineralogy at Maqarin (Jordan)
7.3	Fe-bearing colloids may retard U and other spent fuel components by forming colloids that are filtered from suspension at short distances		
8.2			Analogue studies prediction that most infiltration does not become seepage as observed at Kartchner Caverns, Arizona and Altamira Cave in Spain
8.3	Qualitative evidence of flow diversion around openings in the unsaturated zone independent of climate demonstrated by cave paintings in southern Europe, Egyptian tombs, Buddhist temples		
8.3	Decreases in seepage with decrease in infiltration demonstrated by preservation of fragile human artifacts and organic materials over thousands of years		

Table 15-1. Natural Analogues in This Report and Their Potential Applications to Performance Assessment (cont.)

Section in Natural Analogue Report	Conceptual Model Development (Applied Processes from Natural Analogues)	Use of Specific Parameters in Yucca Mountain TSPA Model	Use for Model Validation of Yucca Mountain Characterization
9.3			Calibration using ITOUGH2 to hydrographs at LPIT yielded parameters consistent with measured data
9.3			Dual-permeability model adequately captured flow but not transport
10.4	Significant dissolution of U may have occurred in groundwaters near Nopal i; also higher dissolution (or more U concentration) during dry season		
10.5	Colloidal transport of U, Th in oxidizing UZ at Steenkampskraal and Koongarra (little at Koongarra)		
11.2	Fluid flow in fractures, as seen in Dixie Valley (USA), Silangkitang (Indonesia) and Wairakei (NZ) geothermal fields		
11.2	Numerical simulation of heat and fluid flow in numerous developed geothermal systems		Confirmation of TOUGH2-based thermal-hydrological reservoir simulations through post-audit history matching of Olkaria (Kenya) and Nesjavellir (Iceland) geothermal fields
11.2	Use of chemical tracers to constrain source of fluids, track movement of fluids, and identify high-permeability flow paths, as conducted at Bulalo (Philippines) geothermal field		
11.2, 11.3	Changes in water chemistry, precipitation of silica and calcite, and reductions in porosity and permeability resulting from boiling, as observed at Waiotapu (NZ), Cerro Prieto (Mexico), and Yellowstone (WY) geothermal fields		
11.2	Precipitation of salts and silica associated with dryout, as observed in Karaha-Telaga Bodas (Indonesia) geothermal field		